Regeneration of dopaminergic neurons in adult zebrafish depends on immune system activation and differs for distinct populations

TITLE: Regeneration of dopaminergic neurons in adult zebrafish depends on immune system activation and differs for distinct populations.

AUTHORS: Lindsey J. Caldwell[1§], Nick O. Davies[1§#], Leonardo Cavone[1], Karolina S. Mysiak[1], Svetlana A. Semenova[2], Pertti Panula[2], J. Douglas Armstrong[3], Catherina G. Becker[1*], Thomas Becker[1*#].

ADDRESSES: [1]Centre for Discovery Brain Sciences, University of Edinburgh, The Chancellor's Building, 49 Little France Crescent, Edinburgh EH16 4SB, UK; [2]Neuroscience Center and Department of Anatomy, University of Helsinki, 00290 Helsinki, Finland; [3]School of Informatics, University of Edinburgh, 10 Crichton Street, Edinburgh EH8 9AB, UK

§ joint first authors; # co-corresponding; * joint senior authors

For correspondence: Nick O. Davies: nck.dvs1@gmail.com; Thomas Becker: thomas.becker@ed.ac.uk.

ABSTRACT:

Adult zebrafish, in contrast to mammals, regenerate neurons in their brain, but the extent and variability of this capacity is unclear. Here we ask whether loss of various dopaminergic neuron populations is sufficient to trigger their functional regeneration. Both sexes of zebrafish were analysed. Genetic lineage tracing shows that specific diencephalic ependymo-radial glial progenitor cells (ERGs) give rise to new dopaminergic (Th^+) neurons. Ablation elicits an immune response, increased proliferation of ERGs and increased addition of new Th^+ neurons in populations that constitutively add new neurons, e.g. diencephalic population 5/6. Inhibiting the immune response attenuates neurogenesis to control levels. Boosting the immune response enhances ERG proliferation, but not addition of Th^+ neurons. In contrast, in populations in which constitutive neurogenesis is undetectable, e.g. the posterior tuberculum and locus coeruleus, cell replacement and tissue integration are incomplete and transient. This is associated with loss of spinal Th^+ axons, as well as permanent deficits in shoaling and reproductive behaviour. Hence, dopaminergic neuron populations in the adult zebrafish brain show vast differences in regenerative capacity that correlate with constitutive addition of neurons and depend on immune system activation.

SIGNIFICANCE STATEMENT

Despite the fact that zebrafish show a high propensity to regenerate neurons in the brain, this study reveals that not all types of dopaminergic neurons are functionally regenerated after specific ablation. Hence, in the same adult vertebrate brain, mechanisms of successful and incomplete

regeneration can be studied. We identify progenitor cells for dopaminergic neurons and show that activating the immune system promotes proliferation of these cells. However, in some areas of the brain this only leads to insufficient replacement of functionally important dopaminergic neurons that later disappear. Understanding the mechanisms of regeneration zebrafish may inform interventions targeting regeneration of functionally important neurons, such as dopaminergic neurons, from endogenous progenitor cells in non-regenerating mammals.

INTRODUCTION

The adult mammalian brain shows very limited neurogenesis after injury or neuronal loss, leading to permanent functional deficits (Peron and Berninger, 2015; Jessberger, 2016). By contrast, the regenerative capacity of the CNS in adult zebrafish after injury is remarkable (Becker and Becker, 2015; Alunni and Bally-Cuif, 2016; Ghosh and Hui, 2016). However, relatively little is known about the capacity for regeneration and functional integration after loss of discrete cell populations in the fully differentiated adult CNS.

To study regeneration of distinct populations of neurons without physical damage, we ablated dopaminergic and noradrenergic neurons using 6-hydroxydopamine (6OHDA), which selectively ablates these neurons across vertebrates (Berg et al., 2011; Tieu, 2011; Matsui and Sugie, 2017; Vijayanathan et al., 2017). In adult zebrafish, the dopaminergic system is highly differentiated. There are 17 distinct dopaminergic and noradrenergic brain nuclei, identified by immunohistochemistry for cytoplasmic Tyrosine hydroxylase (Th) and the related Th2, rate-limiting enzymes in dopamine and noradrenaline synthesis (Chen et al., 2009; Tay et al., 2011). Projections of Th^+ brain nuclei are far-reaching, including long dopaminergic projections to the spinal cord from population 12 in the diencephalon and noradrenergic projections from the locus coeruleus (LC) in the brainstem. These projections are the only Th^+ input to the spinal cord (McLean and Fetcho, 2004a, b; Tay et al., 2011; Kuscha et al., 2012).

Functionally, dopamine, especially from the diencephalo-spinal projection from population 12, has roles in maturation and initiation of motor patterns in developing zebrafish (Thirumalai and Cline, 2008; Lambert et al.,

2012; Reimer et al., 2013; Jay et al., 2015). In addition, dopamine has been linked to anxiety-like behaviour in zebrafish (Tran et al., 2016; Wang et al., 2016). Dopaminergic neurons are constantly generated in the adult diencephalon (Grandel et al., 2006), but it is unclear which populations receive new neurons and how this may change after ablation.

For regeneration of neurons to occur, ependymo-radial glia (ERG) progenitor cells need to be activated. ERGs have a soma that forms part of the ependyma and radial processes that span the entire thickness of the brain. After a CNS injury, these cells are either activated from quiescence or increase their activity in constitutively active adult proliferation zones to regenerate lost neurons (Grandel and Brand, 2013; Becker and Becker, 2015; Alunni and Bally-Cuif, 2016). Activation could occur via damage to the highly branched ERG processes or early injury signals. Remarkably, the microglial/macrophage reaction following a mechanical lesion has been shown to be both necessary and sufficient for regenerative proliferation of ERGs and neurogenesis in the adult zebrafish telencephalon (Kyritsis et al., 2012). The immune response also promotes neuronal regeneration in the spinal cord of larval zebrafish after a lesion (Ohnmacht et al., 2016). Hence, it might also play a role in the regenerative response after discrete neuronal loss without injury.

We find that locally projecting dopaminergic neurons in the diencephalon are regenerated from specific ERGs, whereas large Th^+ neurons with spinal projections are only transiently replaced, associated with permanent and specific functional deficits in shoaling and mating behaviour. Inhibiting the immune response abolished ablation-induced regeneration.

105 Hence, we demonstrate an unexpected heterogeneity in regenerative capacity
106 of functionally important dopaminergic neurons in the adult zebrafish and
107 essential functions of the immune response.
108

MATERIAL AND METHODS

Animals

All fish were kept and bred in our laboratory fish facility according to standard methods (Westerfield, 2000), and all experiments had been approved by the British Home Office. We used wild type (*wik*) and *Tg(olig2:DsRed2)* (Kucenas et al., 2008), abbreviated as *olig2:DsRed*; *Tg(gfap:GFP)* (Bernardos and Raymond, 2006), abbreviated as *gfap*:GFP; *Tg(slc6a3:EGFP)* (Xi et al., 2011), abbreviated as *dat*:GFP, and *Tg(her4.1:TETA-GBD-2A-mCherry)* (Knopf et al., 2010), abbreviated as *her4.3*:mCherry, transgenic reporter lines. Note that zebrafish nomenclature treats *her4.1* and *her4.3* as synonymous (https://zfin.org/ZDB-TGCONSTRCT-110825-6). For genetic lineage tracing, we used *Tg(-3her4.3:Cre-ERT2)* (Tübingen background)(Boniface et al., 2009) crossed with *Tg(actb2:LOXP-mCherry-LOXP-EGFP)* (Ramachandran et al., 2010), as previously described (Skaggs et al., 2014). Adult (> 4 months of age) male and female fish were used for the experiments.

Bath application of substances

For dexamethasone treatment, fish were immersed in 15 mg/L dexamethasone (Sigma-Aldrich, D1756) or vehicle (0.06% DMSO) in system water (Kyritsis et al., 2012). Dexamethasone treatment did not cause any obvious changes in fish behaviour. For lineage tracing experiments, fish were immersed in 1 μM 4-hydroxytamoxifen (Sigma-Aldrich, H6278) in system water with tanks protected from light. Fish were transferred into fresh drug/vehicle every other day.

Intraventricular injections

Fish were anaesthetised in MS222 (Sigma-Aldrich,1:5000 % w/v in PBS) and mounted in a wet sponge to inject the third ventricle from a dorsal approach using a glass capillary, mounted on a micromanipulator. Using sharp forceps, a hole was made into the skull covering the optic tectum and the needle was advanced at a 45° angle from the caudal edge of the tectum into the third ventricle. The capillary was filled with a 10 mM solution of 6OHDA (6-Hydroxydopamine hydrobromide, Sigma-Aldrich, product number: H116) in H_2O and 0.12% of a fluorescent dextran-conjugate (Life Technologies, product number: D34682) to ablate Th^+ cells, or with fluorescently labelled Zymosan A (from *Saccaromyces cerevisiae*) bioparticles at a concentration of 10 mg/mL (Life Technologies, product number: Z23373) to stimulate the microglial response. LTC4 (Cayman Chemicals, product number: 20210) was injected at a concentration of 500 ng/ml in 0.45% ethanol in H_2O. Sham-injected controls were generated by injecting vehicle solutions.

A pressure injector (IM-300 microinjector, Narishige International, Inc. USA) was used to inject 0.5 to 1.0 µL of the solution. The skull is sufficiently translucent to detect a fluorescent dye distributing through the ventricular system. Therefore, we were able to verify successful distribution of the solution throughout the ventricular system under a fluorescence-equipped stereo-microscope. This injection technique only induced a localised microglia reaction surrounding the point where the capillary penetrated the optic tectum, but not close to any of the Th^+ populations of interest.

Intraperitoneal injections

Fish were anaesthetised in MS222 and injected on a cooled surface on their left side with a 30½ G needle. Per application, 25 µl of 16.3mM EdU (Invitrogen) was injected intraperitoneally. EdU was dissolved in 15% DMSO and 30% Danieau's solution in distilled water.

Haloperidol (Sigma-Aldrich, product number: H1512) was injected at a volume of 25 µl and a concentration of 80 µg/ml in PBS for each injection. This roughly equates to 4 mg/kg, twice the concentration shown to be effective in salamanders (Berg et al., 2011).

Quantitative RT-PCR

Brains were dissected without any tissue fixation and sectioned on a vibrating-blade microtome. RNA was isolated from a horizontal section 200 µm thick at the level used for analysis of proliferating ERGs around the ventricle (refer to Fig. 5A for section level) using the RNeasy Mini Kit (Qiagen, 74106). cDNA synthesis was performed using the iScript™ cDNA Synthesis Kit (Bio-Rad, 1708891). Standard RT-PCR was performed using SsoAdvancedTM Universal SYBR® Green Supermix (Bio-Rad, 172-5271). qRT-PCR (annealing temperature 58 °C) was performed using Roche Light Cycler 96 and relative mRNA levels were determined using the Roche Light Cycler 96 SW1 software. Samples were run in duplicates and expression levels were normalized to the level of 18S ribosomal RNA. Primers were designed to span an exon-exon junction using Primer-BLAST. Primer sequences:

184 *tnf*-α: FW 5'-TCACGCTCCATAAGACCCAG-3', RV 5'-
185 GATGTGCAAAGACACCTGGC-3', *il-1β* FW 5'-
186 ATGGCGAACGTCATCCAAGA-3', RV 5'-GAGACCCGCTGATCTCCTTG-3',
187 18S FW 5'- TCGCTAGTTGGCATCGTTTATG-3', RV 5'-
188 CGGAGGTTCGAAGACGATCA-3'.
189
190 HPLC
191 Brains were dissected without any tissue fixation and frozen. HPLC
192 analysis was performed as described (Sallinen et al., 2009).
193
194 Immunohistochemistry
195 We used mouse monoclonal antibody 4C4 (1:50; HPC Cell Cultures,
196 Salisbury, UK, catalogue number: 92092321) to label microglia. The antibody
197 labels microglia in the brain, but not peripheral macrophages (Ohnmacht et
198 al., 2016). We used a chicken antibody to green fluorescent protein (GFP)
199 (1:500; Abcam, Cambridge, MA, USA, designation: ab13970); a mouse
200 monoclonal antibody to the proliferating cell nuclear antigen (PCNA) (1:1000;
201 Dako, Sigma-Aldrich, St Louis, MO, USA, designation: M0879); a mouse
202 monoclonal antibody to tyrosine hydroxylase (Th) (1:1000; Merck Millipore,
203 Billerica, MA, US, designation: MAB318). Suppliers for the appropriate
204 fluorescence or biotin-labelled antibodies were Stratech Scientific, Sydney,
205 Australia and Vector Laboratories, Burlingame, CA, USA, respectively.
206 Dilutions of secondary antibodies followed the manufacturers'
207 recommendations.

Immunofluorescent labelling of 50 µm sections was carried out as previously described (Barreiro-Iglesias et al., 2015). Briefly, brains from perfusion-fixed (4% paraformaldehyde) animals were dissected, sectioned on a vibrating-blade microtome, incubated with primary antibody at 4 °C overnight, washed, incubated in secondary antibody for 45 min at room temperature, washed and mounted in glycerol. All washes were 3 times 15 minutes in PBSTx (0.1% Triton X 100 in PBS).

For colorimetric detection of Th, a biotinylated secondary antibody was used, followed by the ABC reaction using the Vectastain ABC kit (Vector Laboratories, Burlingame, USA) according to the manufacturer's recommendations. The colour was developed using diaminobenzidine solution (1:120 diaminobenzidine; 2 µl/ml of 1% stock $NiCl_2$ and 2 µl/ml of 1% stock $CoSO_4$ in PBS) pre-incubation (30 min at 4°C), followed by addition of 30% hydrogen peroxide. Sections were mounted, dried and counterstained in neutral red staining solution (4% acetate buffer (pH 4.8) and 1% neutral red in dH2O) for 6 min, followed by differentiation in 70% and 95% ethanol.

EdU detection

To detect EdU, we used Click-iT® EdU Alexa Fluor® 488 or 647 Imaging Kits (Molecular Probes) according to the manufacturer's recommendations. Briefly, 50 µm sections from perfusion-fixed brains were incubated in Click-iT reaction buffer for three hours in the dark at room temperature, washed 3 x 10 min in 0.3% PBSTx and once in PBS. After that, sections were mounted in 70% glycerol or underwent immunofluorescent labelling as above.

TUNEL labelling

TUNEL labelling was carried out as described (Reimer et al., 2008) using the *in situ* TMR cell death detection kit (Roche) according to the manufacturer's recommendations. In brief, sections were incubated with reaction mix in the dark at 37°C for 60 min. This was followed by immunolabelling as described above.

Quantification of cells and axons

All counts were carried out with the observer blinded to the experimental condition. For colorimetric immunohistochemistry of Th, cell profiles were counted for individual brain nuclei, identified by neutral red counterstain. Innervation density of labelled axons was semi-quantitatively determined by determining the average pixel brightness for a region of interest using Image J.

In fluorescently labelled sections, cells were stereologically counted in confocal image stacks, as described (Barreiro-Iglesias et al., 2015). To quantify Th/EdU double-labelled cells, all sagittal serial vibrating blade microtome sections (50 µm in thickness) containing the populations in question were scanned on a confocal microscope and numbers of cells were determined by manually going through the image stacks for all sections.

To quantify PCNA or EdU-labelled ERGs, we used one horizontal section (50 µm in thickness) at the levels of the 5/6 population, identified by the characteristic shape of the ventricle.

257 Double-labelling of cells was always assessed in single optical sections
258 (< 2 µm thickness). Fluorescently labelled axons in the spinal cord were
259 quantified using automatic functions in Image J as described (Kuscha et al.,
260 2012).
261
262 Behavioural tests
263 All behaviour tests, comparing between 6OHDA-injected and sham-
264 injected animals, were performed when at least seven days had passed after
265 injection. All recordings were made with a Sony Ex-waveHAD B&W video
266 camera and videos were analysed using Ethovision XT7 tracking software
267 (Noldus, Leesberg, USA), except for shoaling analysis (see below).
268 For the open field test, fish swimming was recoded in a round tank
269 (16.3 cm diameter, 8 cm water depth) for 6 min after 2 minutes acclimatization
270 time. The software calculated the total distance moved and the average
271 velocity of fish.
272 For the light/dark test, a tank (10 cm x 20 cm, 8 cm water depth) was
273 illuminated from below with half of the area blocked from the light. The time
274 spent in the illuminated area was recorded in the 6 minutes immediately
275 following placement of the fish.
276 For the novel tank, test fish were placed in a tank 23 cm x 6 cm, 12 cm
277 water depth, divided into three 4 cm zones) and their time spent in the
278 different depth zones recorded for 6 minutes immediately after the fish were
279 placed.
280 For the shoaling test, groups of four fish were placed into a large tank
281 (45.5 cm x 25 cm, water depth 8 cm) and their swimming recorded for 6 min

after 2 min of acclimatization time. Fish were not selected for sex. Fish were simultaneously tracked and the pairwise Euclidean distance between each pair of fish determined and averaged per frame using commercially available Actual Track software (Actual Analytics, Edinburgh).

To test mating success, pairs of fish were placed into mating tanks (17.5 cm x 10 cm, water depth 6 cm) with a transparent divider in the evening. The next morning, the divider was pulled at lights-on and the fish were allowed to breed for 1 hour. Each pair was bred 4 times every other day. Numbers of fertilized eggs in the clutch and the percentage of successful matings were recorded. A mating attempt was scored as successful, when fertilised eggs were produced.

Statistical analyses

Quantitative data were tested for normality (Shapiro-Wilk test, *p< 0.05) and heteroscedasticity (Levene's test, *p < 0.05) to determine types of statistical comparisons. Variability of values is always given as SEM. Statistical significance was determined using Student's t-test for parametric data (with Welch's correction for heteroscedastic data) or Mann-Whitney U-test for nonparametric data. For multiple comparisons, we used one-way ANOVA with Bonferroni's post-hoc test for parametric homoscedastic data, one-way ANOVA with Welch's correction and Games-Howell post-hoc test for heteroscedastic data, and Kruskall-Wallis test with Dunn's post-test for nonparametric data. The shape of distributions was assessed using a Kolmogorov-Smirnov test (Fig.13). Randomisation was performed by alternating allocation of fish between control and treatment groups. No

experimental animals were excluded from analysis. All relevant data are available from the authors.

311 RESULTS

312

313 Intraventricular injection of 6OHDA ablates specific populations of
314 dopaminergic neurons and locally activates microglia.

315 To ablate dopaminergic and noradrenergic (Th^+) neurons in the
316 absence of damage to tissue and ERG processes, we established an ablation
317 paradigm that relies on intraventricular injections of 6OHDA (Fig.1 A). Of the
318 quantifiable Th^+ cell populations in the brain (Sallinen et al., 2009), we found
319 no effect of 6OHDA injection on cell numbers in populations 2($p=0.104$),
320 7($p=0.587$), 9 ($p=0.302$), 13 ($p=0.342$) and 15/16 ($p=0.989$) at 2 days post-
321 injection (dpi; Fig. 1B). However, there was a 51% loss in population 5/6
322 (control: 484 ± 24 cell profiles; 6OHDA: 235 ± 14 cell profiles), 19% loss of
323 TH^+ cells in population 11 (288 ± 12 in controls vs. 234 ±16 in treated), 96% in
324 population 12 (28 ± 1 in controls vs. 1 ± 0 in treated) and complete loss of
325 noradrenergic neurons in the locus coeruleus (LC; 18 ± 1 in controls vs. zero
326 in treated; Fig. 1B). Higher doses of 6OHDA did not increase loss of Th^+ cells
327 (data not shown). Consistent with Th^+ cell loss, we found a 45% reduction in
328 dopamine levels, but no effect on serotonin ($p = 0.899$) or its metabolites 5-
329 HIAA ($p = 0.965$) and 3-MT ($p = 0.940$) after 6OHDA injection, measured in
330 the whole brain by HPLC (Fig. 1C). There were no obvious correlations
331 between the distance of neurons from the injection site or morphology of the
332 neurons and rates of ablation (see Fig 1A). The failure to ablate other
333 populations is unlikely to be due to lack of diffusion, because the vulnerable
334 LC population is the furthest away from the injection site and other much
335 closer brain nuclei, such as population 7, did not show any cell loss. 6OHDA

loses activity within hours (Ding et al., 2004) and we did not observe overt progressive cell loss at later time points (42 dpi). However, limited delayed cell death cannot be excluded. Hence, we devised an ablation paradigm in which neurons in populations 5/6, 11, 12 and the LC were highly vulnerable to 6OHDA.

To determine whether 6OHDA injections led to specific death of Th^+ neurons and activation of an immune response, we combined TUNEL labelling and immunohistochemistry for microglia using the 4C4 antibody, which selectively labels microglial cells (Becker and Becker, 2001; Ohnmacht et al., 2016) in a reporter fish for dopaminergic neurons (*dat*:GFP) (Xi et al., 2011) at 12 h post-injection. This indicated selective appearance of $TUNEL^+$/*dat:*GFP^+ profiles in the vulnerable populations, but not in the non-ablated populations or in areas not labelled by the transgene (Fig. 1D; see also Fig. 8A for localised microglia reaction after 6OHDA treatment). Some microglial cells engulfed $TUNEL^+$/*dat:*GFP^+ profiles, indicating activation of microglia (Fig. 1E). Quantification shows that the density of microglial cells was doubled in these areas (Fig. 1F). About half of the cells were associated with TUNEL signal, whereas in controls, only very few cells were associated with debris. Associations of all three labels (4C4 / TUNEL / *dat:*GFP) were rare (Fig. 1F). We interpret this to be a consequence of dying Th^+ cells losing GFP labelling very quickly. Hence, 6OHDA only leads to death of circumscribed dopaminergic cell populations and elicits a localised microglial response.

Cell replacement patterns differ between dopaminergic cell populations.

To analyse whether lost Th^+ neurons were replaced, we assessed Th^+ cell numbers relative to controls without ablation for up to 540 dpi (1.5 years post-injection) of the toxin. The relatively small loss of cells in population 11 was compensated for at 42 dpi (not shown). In population 5/6, numbers were increased compared to 2 dpi, but were still lower than in controls by 42 dpi. However, at 180 dpi, Th^+ cell numbers were even slightly increased over controls. At 540 dpi, numbers were similar to age-matched controls ($p > 0.999$) (Fig. 2A-F). In contrast, in population 12 and the LC, Th^+ neuron numbers were never fully recovered. There was a small and transient recovery in cell numbers in these populations at 42 dpi, but by 540 dpi there were hardly any neurons present in population 12 and the LC (Fig. 2G-R). This indicates differential potential for cell replacement for different populations of dopaminergic neurons.

To determine whether restored dopaminergic neurons re-innervated their former target areas, we analysed a terminal field ventral to the predominantly locally projecting population 5/6 (Tay et al., 2011), which showed regeneration of cell bodies. After ablation, the density of Th^+ innervation of this terminal field, measured semi-quantitatively by relative labelling intensity, was significantly reduced, compared to controls. This was still the case at 180 dpi, even though cell replacement had been almost completed by 42 days dpi. At 540 dpi, the axon density in 6OHDA-injected fish was comparable to other time points, though just not statistically different from age-matched controls ($p = 0.0661$). This is likely due to the higher

variability observed in aged fish. This suggests slow if any restoration of local projections (Fig. 3A-E).

Since population 12 and the LC, which show little cell replacement, provide all Th^+ innervation to the spinal cord (McLean and Fetcho, 2004a, b; Kuscha et al., 2012), we assessed innervation of Th^+ axons of the spinal cord. In animals without ablation, we always observed Th^+ axons in the spinal cord at a midthoracic level (n = 26). Between 2 and 540 dpi, these axons were almost completely absent from the spinal cord in 6OHDA injected animals (Fig. 3F-H). Hence the entire Th^+ projection to the spinal cord was ablated by 6OHDA treatment and never regenerated.

Capacity for enhanced addition of new dopaminergic neurons after ablation correlates with presence of constitutive neurogenesis for different populations

To determine how dopaminergic neurons were replaced after ablation we assessed whether neurogenesis of dopaminergic neurons could be observed and whether ablation of dopaminergic neurons changed generation rates. To that aim, we injected EdU daily for 7 days after 6OHDA injection, to maximise progenitor labelling. We analysed the number of Th^+/EdU^+ neurons at 6 weeks post-injection, allowing sufficient time for differentiation of Th^+ neurons (Fig. 4A). Even in the non-ablated situation, a low number of double-labelled neurons was observed in populations that were capable of neuron replacement, that is in populations 5/6, 8 and 11 (Fig. 4B,E-G). For the countable populations 5/6 and 11, double-labelled cells represented 1.4% and 5.7%, respectively, of the average number of Th^+ cells in these populations.

410 This indicates that dopaminergic neurons are constantly added to specific
411 populations at a low rate.
412 After ablation, the number of double-labelled cells was increased 5-fold
413 in population 5/6 to 7.0% of all TH^+ cells (Fig. 4C,D,E), compared to sham-
414 injected animals. A similar non-significant trend was present in populations 8
415 ($p = 0.073$) and 11 ($p = 0.186$) (Fig. 4F,G). In population 11, 15.2% Th^+ cells
416 were double-labelled after 6OHDA injection. Hence, ablation of Th^+ cells
417 increases the rate of addition of new neurons to regenerating populations.
418 In contrast, in population 12 and the LC, which did not show strong
419 replacement of Th^+ neurons after 6OHDA injection in our histological analysis
420 above, we did also not observe EdU^+/Th^+ neurons without or with ablation
421 (Fig. 4H,I). Hence, differences in Th^+ neuron replacement capacity correlate
422 with differences in constitutive neurogenesis for distinct populations.
423
424 <u>New dopaminergic neurons are derived from ERGs</u>
425 New Th^+ cells are likely derived from local ERGs. The ventricle close to
426 the 5/6 population is lined by cells with radial processes spanning the entire
427 thickness of the brain. Most of these cells are labelled by *gfap*:GFP, indicating
428 their ERG identity (Kyritsis et al., 2012), and Th^+ cells are located close to
429 ERG processes (Fig. 5A,B). Using PCNA labelling, we find that some of the
430 ERGs proliferate in the untreated brain, consistent with a function in
431 maintaining dopaminergic and other cell populations (cf. Fig. 11E,F).
432 To determine whether new Th^+ cells are derived from ERGs we used
433 genetic lineage tracing with a *Tg(-3her4.3:Cre-ERT2)* x *Tg(actb2:LOXP-*
434 *mCherry-LOXP-EGFP)* double-transgenic fish (Boniface et al., 2009). In this

fish, tamoxifen-inducible Cre is driven by the regulatory sequences of the *her4.3* gene. *her4.3* is specifically expressed in zebrafish ERGs (Kroehne et al., 2011). The second transgene leads to expression of GFP in ERGs and their progeny after Cre-recombination. We found a strong overlap between *gfap*:GFP and *her4.3*:mCherry labelling, indicating that the driver targets the appropriate cell population (Fig. 5C).

We incubated animals in tamoxifen for 6 days to induce recombination in ERGs, injected 6OHDA and waited for another 42 days for histological analysis. In animals without previous tamoxifen application, we did not observe any GFP^+ cells. In tamoxifen-incubated animals, mostly ERGs were labelled at different densities, indicating variable recombination rates. Variable recombination rates could have resulted from variability of transgene expression in individual fish. Even though we used an extensive 4OHT incubation protocol (Ramachandran et al., 2010), we cannot exclude inefficient diffusion as another reason for variable recombination. In animals in which high recombination rates were achieved, we found GFP^+/Th^+ cells after the chase period, indicating that ERGs gave rise to dopaminergic neurons (Fig. 5D-F). However, we cannot exclude additional sources for new Th^+ neurons that might be active during physiological or ablation-induced addition of these neurons.

Generation of new Th^+ cells depends on immune system activation

To test whether the observed activation of microglial cells (cf. Fig. 1D) was necessary for Th^+ cell regeneration, we inhibited the immune reaction using dexamethasone bath application (Kyritsis et al., 2012) and analysed

460 effects on ERG proliferation and Th+ cell generation. Dexamethasone is an
461 artificial glucocorticoid with effective immuno-suppressive features, but it also
462 affects other cellular processes (Juszczak and Stankiewicz, 2018; Ronchetti
463 et al., 2018). qRT-PCR for principal pro-inflammatory cytokines *il-1β* and *tnf*-α
464 on horizontal brain sections, comprising population 5/6, showed an ablation-
465 induced increase in the expression of these cytokines in control fish that was
466 consistent with the morphological activation of microglia. This increase was
467 completely inhibited in the presence of dexamethasone ($p = 0.918$ and 0.9982
468 respectively, compared to sham injected), indicating that treatment was
469 efficient (Fig. 6A,B).

470 To quantify ERG proliferation, we incubated fish with dexamethasone
471 from 1-13 dpi of 6OHDA and injected EdU at 11 dpi, followed by analysis at
472 13 dpi (Fig. 6C). In the vicinity of the 5/6 population, most ERGs express *gfap*.
473 Some of these co-express *olig2* and some express only *olig2*, as indicated by
474 reporter fish double-transgenic for *gfap*:GFP and *olig2*:DsRed (Fig. 6D,E).
475 Without dexamethasone, ERGs that were only *gfap*:GFP$^+$ showed increased
476 rates of EdU incorporation after 6OHDA injection compared to sham-injected
477 animals (Fig. 6F). Whereas ERGs that were only *olig2*:DsRed$^+$ showed a
478 similar trend($p = 0.079$; Fig. 6G), double-labelled ERGs did not show any
479 6OHDA-induced effect on proliferation ($p = 1$; Fig. 6H). This shows that
480 specific ERGs increase proliferation after ablation of Th$^+$ neurons.

481 Dexamethasone had no significant effect on proliferation rates of any
482 ERG subtype in sham-injected controls, indicating that it likely did not
483 influence ERG proliferation directly(*gfap*:GFP: $p = 0.087$; *olig2*:DsRed: $p = 1$;
484 *gfap*:GFP*/olig2*:DsRed: $p = 0.211$). In contrast, increased proliferation rates in

485 only *gfap*:GFP$^+$ ERGs of animals injected with 6OHDA were reduced to those
486 seen in constitutive proliferation. This was statistically significant (Fig. 6F).
487 ERGs that were only *olig2*:DsRed$^+$ showed a similar trend ($p = 0.092$; Fig.
488 6G). This showed that only ablation-induced proliferation of *gfap*:GFP$^+$ ERGs
489 depended on immune system activation.
490 To determine whether this early suppression of the immune response
491 and ERG proliferation had consequences for the addition of newly generated
492 Th$^+$ cells to population 5/6, we incubated animals for 14 days with
493 dexamethasone after ablation and analysed Th$^+$ neuron addition at 42 days
494 after ablation. This showed lower numbers of Th$^+$/EdU$^+$ neurons and lower
495 overall numbers of Th$^+$ neurons compared to 6OHDA treated animals without
496 dexamethasone treatment (Fig. 7A-E). Hence, dexamethasone treatment
497 early after ablation led to reduced rates of ERG proliferation and later Th$^+$
498 neuron addition to population 5/6. This shows that regenerative neurogenesis
499 depends on immune system activation.
500
501 <u>Augmenting the immune response enhances ERG proliferation, but not</u>
502 <u>dopaminergic neuron regeneration</u>
503 To determine whether the immune response was sufficient to induce
504 dopaminergic cell generation and could be augmented to boost regeneration
505 we used Zymosan A injections into the ventricle, compared to sham-injected
506 controls and 6OHDA injection (Kyritsis et al., 2012). Zymosan A are glycan
507 complexes prepared from yeast cell walls that directly interact with
508 macrophages/microglia and stimulates the inflammatory response (Novak and
509 Vetvicka, 2008). However, other cells may also react to this stimulus.

6OHDA, which selectively ablates dopaminergic cells due to its dependency on the presence of dopamine transporter (Gonzalez-Hernandez et al., 2004), only led to a local increase of 4C4 immunoreactivity, secondary to the specific cell death of dopaminergic neurons. Hence, microglia activation was clustered in specific brain nuclei, e.g. in the 5/6 population (Fig. 8A). In contrast, due to its direct action on immune cells, our ventricular injections of Zymosan led to a strong general increase in immunoreactivity for the microglia marker 4C4 that lasted for at least 3 days (Fig. 8A). qRT-PCR measurements indicated a massive 20-fold increase of *tnf*-α mRNA expression and a 31-fold increase of *il-1β* mRNA expression at 12 hours post-injection (hpi; Fig. 8B). In the presence of dexamethasone, Zymosan-induced increases in *tnf*-α and *il-1β* mRNA expression were strongly inhibited. This supports action of both Zymosan and dexamethasone on the immune response. Hence, Zymosan injections can be used to boost the inflammatory reaction.

Without prior ablation of Th^+ neurons, Zymosan injections led to increased proliferation of only *gfap*:GFP^+ and only *olig2*:$DsRed^+$ ERGs, but not of double-labelled ERGs (ANOVA: $p = 0.45$) compared to untreated controls (Zymosan A injections at 5 and 10 days after 6OHDA injection, EdU application at 11 dpi, analysis at 13 dpi; Fig. 8C-G). After 6OHDA-mediated cell ablation, Zymosan treatment showed a trend to further enhance proliferation of only *gfap*:GFP^+ ERGs compared to fish only treated with 6OHDA (Fig. 8E). However, this relatively weak additive effect was not statistically significant ($p = 0.103$). Hence, Zymosan increased proliferation of

mainly *gfap*:GFP$^+$ ERGs independently of an ablation, and potentially slightly increased proliferation beyond levels induced by 6OHDA treatment alone.

To investigate whether Zymosan treatment was able to improve regeneration of Th$^+$ neurons after ablation, we analysed the number of EdU$^+$/Th$^+$ and the total number of Th$^+$ neurons after 6OHDA induced ablation in the same experimental timeline as above. We did not observe any changes in EdU$^+$/Th$^+$ ($p = 0.193$) and overall numbers of Th$^+$ cells ($p = 0.687$) compared to animals that only received 6OHDA injections (Fig. 9A-E). Hence, Zymosan treatment was sufficient to increase ERG proliferation but insufficient to boost regeneration of Th$^+$ neurons.

To determine whether manipulations of immune signalling would interfere with constitutive addition of new Th+ cells to the 5/6 population, we compared numbers of EdU$^+$/Th$^+$ and overall numbers of Th$^+$ neurons at 42 days after Zymosan (a sham injection followed by two injections of Zymosan at 5 and 10 dpi) or application of dexamethasone (sham injection followed by incubation from 1-15 dpi), as before, but without 6OHDA injection (Fig. 10A-C). Neither treatment changed numbers of newly generated (Fig. 10D) or overall numbers of Th+ cells (Zymosan: $p = 0.918$; dexamethasone: $p = 0.110$; Fig. 10E). Hence, constitutive addition of Th$^+$ cells is not affected by immune signals.

<u>LTC4 injections or inhibition of dopamine signalling did not boost ERG proliferation.</u>

To dissect whether the effect of immune system stimulation on ERG proliferation may have been mediated by leukotriene C4 (LTC4), as in the

559 mechanically injured telencephalon (Kyritsis et al., 2012), we injected animals
560 with the compound. This elicited a weak microglia response after 3 daily
561 injections, as shown by 4C4 immunohistochemistry (Fig. 11A-C), but
562 proliferation of ERGs, as measured by counting $PCNA^+$ cells that were
563 gfap:GFP^+ and/or olig2:$DsRed^+$ was not altered ($p = 0.4286$; Fig. 11D-G). This
564 suggests possible brain region-specific mechanisms of ERG proliferation.
565 To test whether reduced levels of dopamine after cell ablation (cf. Fig
566 1D) might also trigger the increase in ERG proliferation, as in the salamander
567 midbrain (Berg et al., 2011), we used extensive (see Material and Methods)
568 injections of the dopamine D2-like receptor antagonist Haloperidol, which is
569 effective in zebrafish (Reimer et al., 2013), to mimic reduced dopamine levels
570 in animals without ablation. However, this did not increase ventricular
571 proliferation compared to sham-injected control animals($p = 0.425$; Fig. 12A-
572 C), suggesting the possibility that reduced dopamine levels may not be
573 sufficient to trigger progenitor cell proliferation.
574
575 Ablation of dopaminergic neurons leads to specific functional deficits
576 To determine whether loss of Th^+ neurons had consequences for the
577 behaviours of the fish, and whether these would be recovered after
578 regeneration, we first recorded individual swimming activity in a round arena
579 for 6 minutes at 7 days after ablation of fish that received 6OHDA injections
580 and sham-injections. No differences were observed in the distance moved (p
581 $= 0.259$) and velocity ($p = 0.137$) or the preference of fish for the periphery or
582 inner zone of the arena (Fig. 13A-C and not shown). This indicated that
583 swimming capacity and patterns were not overtly affected by the ablation.

584 We used tests of anxiety-like behaviours, namely the novel tank test, in
585 which fish initially prefer to stay at the bottom of the unfamiliar new tank, and
586 the light/dark choice test (Blaser and Gerlai, 2006; Blaser and Rosemberg,
587 2012; Stewart et al., 2012), in which fish stay most of the time in the dark
588 compartment. Indeed, fish in all groups showed strong preferences for the
589 bottom of the tank or the dark compartment, respectively, indicating the
590 expected behaviours. However, fish did not show any differences in behaviour
591 after 6OHDA induced ablation of Th^+ neurons ($p = 0.147$; Fig. 13D-G). Hence,
592 we could not detect effects of Th^+ cell ablation on anxiety-like behaviours.
593 To test movement coordination, we analysed shoaling behaviour of the
594 fish. Putting 4 fish together into a tank lets them exhibit shoaling, a natural
595 behaviour to swim close to their conspecifics (Engeszer et al., 2004). This
596 behaviour requires complex sensory-motor integration to keep the same
597 average distance from each other. We found that shoals made up of fish
598 treated with 6OHDA swam at an average inter-individual distance that was
599 twice as large as that in control shoals at 7, 42 and 180 days post-injection
600 (Fig. 14A,B). Hence ablation of Th^+ neurons impaired shoaling behaviour and
601 this behaviour was not recovered within 180 days dpi.
602 We reasoned that if manoeuvring of fish was impaired by ablation of
603 specific Th^+ cells, mating behaviour, which requires coordinated swimming of
604 a male and female, might also be affected. Alternatively, reproductive
605 functions could directly be influenced by dopamine (Pappas et al., 2010).
606 Indeed, ablation of Th^+ cells in both male and females led to a reduced rate of
607 successful matings and 84% fewer fertilised eggs laid than in control pairs
608 over four mating events. Combining the same control females with the

609 6OHDA treated males and vice versa allowed intermediate egg production
610 and mating success in both groups, indicating that male or female
611 reproductive functions were not selectively affected (Fig. 14C-E). Hence,
612 mating success was only strongly impaired when both males and females
613 lacked specific Th^+ neurons. This supports the notion that swimming
614 coordination was permanently affected by the lack of regeneration in
615 population 12 and the LC.

DISCUSSION

Our results show that after ablation, Th$^+$ neurons in some populations are replaced by newly formed neurons. Th$^+$ neurons are derived from specific ERGs, which increase proliferation after ablation in the adult zebrafish brain. This regeneration depends on immune system activation. In contrast, Th$^+$ neuron populations with long spinal projections only show sparse and transient replacement of neurons and never recover their spinal projections. Consequently, deficits in shoaling and mating behaviours associated with these anatomical defects never recover (schematically summarized in Fig. 15).

Th$^+$ neurons are regenerated from specific ERG progenitors after ablation

We observed a regenerative response after ablation of a subset of Th$^+$ neurons, defined by an increased number of Th$^+$ cells and ERGs labelled with a proliferation marker. Genetic lineage tracing showed that ERGs gave rise to at least some new Th$^+$ neurons. However, we cannot exclude contributions from unknown progenitors or trans-differentiation of other neurons as a source for new dopaminergic neurons. Hence, ablation of Th$^+$ neurons is sufficient to elicit a regenerative reaction in ERG progenitor cells and protracted replacement of Th$^+$ neurons.

Not all diencephalic ERGs may take part in regenerative neurogenesis of dopaminergic neurons. We find previously unreported heterogeneity in gene expression and proliferative behaviour of these cells. While *gfap*:GFP$^+$ (overlapping with the ERGs labelled by genetic lineage tracing) and

641 *olig2*:DsRed$^+$ ERGs showed increases in proliferation in response to Th$^+$ cell
642 ablation or Zymosan injection, those that expressed both transgenes did not.
643 This indicates that only specific ERGs may act as progenitor cells in a
644 regeneration context. Interestingly, in salamanders, ERGs that do not
645 contribute to constitutive neurogenesis are recruited for neurogenesis after
646 ablation of Th$^+$ cells (Berg et al., 2010). *Gfap* and *olig2* co-expressing ERGs in
647 the zebrafish diencephalon may represent an example of an ERG population
648 that cannot be recruited for neurogenesis. Specific repressors of proliferative
649 activity, such as high notch pathway activity, could be a feature of these cells
650 (Dias et al., 2012; Alunni et al., 2013; Than-Trong et al., 2018). Identifying the
651 unique molecular properties of these cells will therefore be an important task
652 for future studies.

653 In previous ablation experiments in larvae, different observations were
654 made depending on the ablated cell populations. Either enhanced proliferation
655 and replacement of neurons (McPherson et al., 2016) or no reaction and long-
656 term reduction in neuron number (Godoy et al., 2015) has been reported. This
657 underscores our findings that different populations of dopaminergic neurons
658 are not regenerated to the same extent, even in larvae that show higher
659 general proliferative activity than adults. Our observation supports that loss of
660 Th$^+$ cells leads to increased proliferation of progenitor cells and replacement
661 of specific dopaminergic neuron populations.

662

663 *The immune response is necessary for regeneration of Th$^+$ cells*

664 We find that inhibiting the immune response after ablation leads to
665 reduced proliferation in the ventricular zone and fewer new Th$^+$ neurons.

Interestingly, only ablation-induced ERG proliferation was affected by this treatment, consistent with findings for the zebrafish telencephalon (Kyritsis et al., 2012). It has been proposed that different molecular mechanisms are involved in constitutive and regenerative neurogenesis (Kizil et al., 2012). However, the immune-mediator LTC4, reported to promote the immune-dependent progenitor proliferation in the zebrafish telencephalon (Kyritsis et al., 2012), did not elicit proliferation of ERGs in our experiments in the diencephalon, suggesting regional differences of immune to ERG signalling.

Alternatively, ERGs could be de-repressed in their activity by the observed reduction of dopamine levels in the brain. This has been demonstrated to be the case in the midbrain of salamanders (Berg et al., 2011). However, injecting haloperidol into untreated fish to mimic reduced levels of dopamine after ablation did not lead to increased ERG proliferation in the brain of zebrafish. This points to potential species-specific differences in the control of progenitor cell proliferation between zebrafish and salamanders.

Remarkably, boosting the immune reaction with Zymosan was sufficient to enhance ERG proliferation, but was insufficient to increase number of new Th^+ neurons in animals with and without prior ablation of Th^+ neurons. This suggests that additional factors, not derived from the immune system, may be necessary for Th^+ neuron differentiation and replacement.

What are the reasons for differential regeneration of dopaminergic neuron populations?

Constitutive neurogenesis we observe in specific brain nuclei correlates with regenerative success. For example, there is ongoing addition

691 of Th^+ cells in the regeneration-competent 5/6 population without any ablation,
692 but this is not detectable in the non-regenerated populations 12 and LC. We
693 speculate that in brain nuclei that constitutively integrate new neurons, factors
694 that support integration of new neurons, such as neurotrophic factors and
695 axon guidance molecules might be present, whereas these could have been
696 developmentally down-regulated in populations that do not add new neurons
697 in adults. Integration promoting factors may be rate-limiting for regeneration.
698 Alternatively, new neurons may fail to integrate into the network and
699 perish. This may be pronounced for population 12 and the LC, which show
700 complex axon projections (Tay et al., 2011). Some dopaminergic cells
701 managed to repopulate population 12 and LC, but they did not persist. These
702 populations have neurons with particularly long axons that are led by complex
703 guidance molecule patterns, e.g. to the spinal cord during development
704 (Kastenhuber et al., 2009). These patterns may have disappeared in adults
705 and thus explain failure of these neurons to re-innervate the spinal cord.
706 Some long-range axons can successfully navigate the adult zebrafish brain,
707 such as regenerating optic axons (Wyatt et al., 2010), but particular
708 populations of axons descending to the spinal cord do not readily regenerate
709 (Becker et al., 1998; Bhatt et al., 2004). This correlates with constitutive
710 neurogenesis in the optic system, but not in the descending brainstem
711 projection.
712
713 *Specific ablation of circumscribed Th^+ populations offers clues to their*
714 *function*

715 The long-lasting loss of about 28 dopaminergic neurons in population
716 12 and of 18 noradrenergic neurons in the LC is associated with highly
717 specific functional deficits in shoaling and mating, but not overall locomotion
718 or anxiety-like behaviours. Previous studies showed reduced overall
719 locomotion after application of 6OHDA in adult zebrafish. However, in these
720 studies, application routes were different, creating larger ablation in the brain
721 (Vijayanathan et al., 2017) or peripheral rather than central lesions (Anichtchik
722 et al., 2004).

723 Among the lost neurons, population 12 contains the neurons that give
724 rise to the evolutionarily conserved diencephalo-spinal tract, providing the
725 entire dopaminergic innervation of the spinal cord in most vertebrates (Tay et
726 al., 2011). Loss of this tract in larval zebrafish leads to hypo-locomotion, due
727 to a reduction in the number of swimming bouts (Thirumalai and Cline, 2008;
728 Jay et al., 2015). Large scale ablation of diencephalic dopaminergic neurons
729 in larvae also led to motor impairments (Lam et al., 2005). We speculate that
730 in adults, dopamine in the spinal cord, which is almost completely missing
731 after ablation, may modulate initiation of movement changes necessary for
732 efficient shoaling and mating behaviour. However, descending dopaminergic
733 projections also innervate the sensory lateral line (Bricaud et al., 2001; Jay et
734 al., 2015). Altered sensation of water movements could thus also contribute to
735 impaired ability to manoeuvre. Moreover, population 12 neurons have
736 ascending projections (Tay et al., 2011) that could also be functionally
737 important. We can also not exclude that some ablated dopaminergic neurons
738 escaped our analysis but contributed to functional deficits.

739 Altered shoaling behaviour (Scerbina et al., 2012) and anxiety-like
740 behaviour (Tran et al., 2016; Wang et al., 2016) has previously been
741 correlated with alterations of the dopaminergic system, but not pinpointed to
742 specific neuronal populations. Our results support that the fewer than 50
743 neurons that form the descending dopaminergic and noradrenergic
744 projections are involved in shoaling behaviour, but not anxiety-like behaviour,
745 as has been found for global manipulations of dopamine (Kacprzak et al.,
746 2017).
747 Dopamine-dependent behaviours can be recovered following
748 regeneration of dopaminergic neurons. For example, in larval zebrafish,
749 swimming frequency is normalised again after ablation and regeneration of
750 hypothalamic dopaminergic neurons (McPherson et al., 2016). In
751 salamanders, amphetamine-inducible locomotion is recovered, correlated with
752 regeneration of Th^+ neurons after 6OHDA-mediated ablation (Parish et al.,
753 2007). Here we show that regeneration of specific Th^+ neurons that project to
754 the spinal cord is surprisingly limited in adult zebrafish and not functionally
755 compensated, which leads to permanent functional deficits in a generally
756 regeneration-competent vertebrate.
757
758 *Conclusion*
759 Specific Th^+ neuronal populations in adult zebrafish show an
760 unexpected heterogeneity in their capacity to be regenerated from specific
761 progenitor populations. This system is useful to dissect mechanisms of
762 successful and unsuccessful functional neuronal regeneration in the same
763 model, and we show here that the immune response is critical for

regeneration. Ultimately, manipulations of immune mechanisms in conjunction with pro-differentiation factors may be used to activate pro-regenerative mechanisms also in mammals to lead to generation and functional integration of new dopaminergic neurons.

ACKNOWLEDGEMENTS

We thank Drs Bruce Appel, Marc Ekker, Daniel Goldman, and Pamela Raymond for transgenic fish, Joe Finney for data analysis and Stephen West for discussions. Supported by BBSRC (BB/M003892/1 to CGB and TB), an MRC DTG PhD studentship (to NOD), a BBSRC Eastbio PhD studentship (to LJC), and a grant from Sigrid Juselius Foundation to SS and PP.

AUTHOR CONTRIBUTION

Conceptualization, NOD, LJC, CGB, and TB; Investigation, NOD, LJC, LC, SAS, KSM, PP and JDA; Writing: CGB and TB.

CONFLICT OF INTEREST STATEMENT

JDA is the founding director of Actual Analytics Ltd.

783 REFERENCES

784 Alunni A, Bally-Cuif L (2016) A comparative view of regenerative
785 neurogenesis in vertebrates. Development 143:741-753.
786 Alunni A, Krecsmarik M, Bosco A, Galant S, Pan L, Moens CB, Bally-Cuif L
787 (2013) Notch3 signaling gates cell cycle entry and limits neural stem
788 cell amplification in the adult pallium. Development 140:3335-3347.
789 Anichtchik OV, Kaslin J, Peitsaro N, Scheinin M, Panula P (2004)
790 Neurochemical and behavioural changes in zebrafish Danio rerio after
791 systemic administration of 6-hydroxydopamine and 1-methyl-4-phenyl-
792 1,2,3,6-tetrahydropyridine. J Neurochem 88:443-453.
793 Barreiro-Iglesias A, Mysiak KS, Scott AL, Reimer MM, Yang Y, Becker CG,
794 Becker T (2015) Serotonin Promotes Development and Regeneration
795 of Spinal Motor Neurons in Zebrafish. Cell Rep 13:924-932.
796 Becker CG, Becker T (2015) Neuronal regeneration from ependymo-radial
797 glial cells: cook, little pot, cook! Dev Cell 32:516-527.
798 Becker T, Becker CG (2001) Regenerating descending axons preferentially
799 reroute to the gray matter in the presence of a general
800 macrophage/microglial reaction caudal to a spinal transection in adult
801 zebrafish. J Comp Neurol 433:131-147.
802 Becker T, Bernhardt RR, Reinhard E, Wullimann MF, Tongiorgi E, Schachner
803 M (1998) Readiness of zebrafish brain neurons to regenerate a spinal
804 axon correlates with differential expression of specific cell recognition
805 molecules. J Neurosci 18:5789-5803.

806 Berg DA, Kirkham M, Wang H, Frisen J, Simon A (2011) Dopamine controls
807 neurogenesis in the adult salamander midbrain in homeostasis and
808 during regeneration of dopamine neurons. Cell Stem Cell 8:426-433.
809 Berg DA, Kirkham M, Beljajeva A, Knapp D, Habermann B, Ryge J, Tanaka
810 EM, Simon A (2010) Efficient regeneration by activation of
811 neurogenesis in homeostatically quiescent regions of the adult
812 vertebrate brain. Development 137:4127-4134.
813 Bernardos RL, Raymond PA (2006) GFAP transgenic zebrafish. Gene Expr
814 Patterns 6:1007-1013.
815 Bhatt DH, Otto SJ, Depoister B, Fetcho JR (2004) Cyclic AMP-induced repair
816 of zebrafish spinal circuits. Science 305:254-258.
817 Blaser R, Gerlai R (2006) Behavioral phenotyping in zebrafish: comparison of
818 three behavioral quantification methods. Behav Res Methods 38:456-
819 469.
820 Blaser RE, Rosemberg DB (2012) Measures of anxiety in zebrafish (Danio
821 rerio): dissociation of black/white preference and novel tank test. PLoS
822 One 7:e36931.
823 Boniface EJ, Lu J, Victoroff T, Zhu M, Chen W (2009) FIEx-based transgenic
824 reporter lines for visualization of Cre and Flp activity in live zebrafish.
825 Genesis 47:484-491.
826 Bricaud O, Chaar V, Dambly-Chaudiere C, Ghysen A (2001) Early efferent
827 innervation of the zebrafish lateral line. J Comp Neurol 434:253-261.
828 Chen YC, Priyadarshini M, Panula P (2009) Complementary developmental
829 expression of the two tyrosine hydroxylase transcripts in zebrafish.
830 Histochemistry and cell biology 132:375-381.

831 Dias TB, Yang YJ, Ogai K, Becker T, Becker CG (2012) Notch signaling
832 controls generation of motor neurons in the lesioned spinal cord of
833 adult zebrafish. J Neurosci 32:3245-3252.
834 Ding YM, Jaumotte JD, Signore AP, Zigmond MJ (2004) Effects of 6-
835 hydroxydopamine on primary cultures of substantia nigra: specific
836 damage to dopamine neurons and the impact of glial cell line-derived
837 neurotrophic factor. J Neurochem 89:776-787.
838 Engeszer RE, Ryan MJ, Parichy DM (2004) Learned social preference in
839 zebrafish. Curr Biol 14:881-884.
840 Ghosh S, Hui SP (2016) Regeneration of Zebrafish CNS: Adult Neurogenesis.
841 Neural plasticity 2016:5815439.
842 Godoy R, Noble S, Yoon K, Anisman H, Ekker M (2015) Chemogenetic
843 ablation of dopaminergic neurons leads to transient locomotor
844 impairments in zebrafish larvae. J Neurochem 135:249-260.
845 Gonzalez-Hernandez T, Barroso-Chinea P, De La Cruz Muros I, Del Mar
846 Perez-Delgado M, Rodriguez M (2004) Expression of dopamine and
847 vesicular monoamine transporters and differential vulnerability of
848 mesostriatal dopaminergic neurons. J Comp Neurol 479:198-215.
849 Grandel H, Brand M (2013) Comparative aspects of adult neural stem cell
850 activity in vertebrates. Dev Genes Evol 223:131-147.
851 Grandel H, Kaslin J, Ganz J, Wenzel I, Brand M (2006) Neural stem cells and
852 neurogenesis in the adult zebrafish brain: origin, proliferation dynamics,
853 migration and cell fate. Dev Biol 295:263-277.

854 Jay M, De Faveri F, McDearmid JR (2015) Firing dynamics and modulatory
855 actions of supraspinal dopaminergic neurons during zebrafish
856 locomotor behavior. Curr Biol 25:435-444.
857 Jessberger S (2016) Neural repair in the adult brain. F1000Research 5.
858 Juszczak GR, Stankiewicz AM (2018) Glucocorticoids, genes and brain
859 function. Prog Neuropsychopharmacol Biol Psychiatry 82:136-168.
860 Kacprzak V, Patel NA, Riley E, Yu L, Yeh JJ, Zhdanova IV (2017)
861 Dopaminergic control of anxiety in young and aged zebrafish.
862 Pharmacology, biochemistry, and behavior 157:1-8.
863 Kastenhuber E, Kern U, Bonkowsky JL, Chien CB, Driever W, Schweitzer J
864 (2009) Netrin-DCC, Robo-Slit, and heparan sulfate proteoglycans
865 coordinate lateral positioning of longitudinal dopaminergic
866 diencephalospinal axons. J Neurosci 29:8914-8926.
867 Kizil C, Kyritsis N, Dudczig S, Kroehne V, Freudenreich D, Kaslin J, Brand M
868 (2012) Regenerative neurogenesis from neural progenitor cells
869 requires injury-induced expression of Gata3. Dev Cell 23:1230-1237.
870 Knopf F, Schnabel K, Haase C, Pfeifer K, Anastassiadis K, Weidinger G
871 (2010) Dually inducible TetON systems for tissue-specific conditional
872 gene expression in zebrafish. Proc Natl Acad Sci USA 107:19933-
873 19938.
874 Kroehne V, Freudenreich D, Hans S, Kaslin J, Brand M (2011) Regeneration
875 of the adult zebrafish brain from neurogenic radial glia-type
876 progenitors. Development 138:4831-4841.

877 Kucenas S, Takada N, Park HC, Woodruff E, Broadie K, Appel B (2008) CNS-
878 derived glia ensheath peripheral nerves and mediate motor root
879 development. Nat Neurosci 11:143-151.
880 Kuscha V, Barreiro-Iglesias A, Becker CG, Becker T (2012) Plasticity of
881 tyrosine hydroxylase and serotonergic systems in the regenerating
882 spinal cord of adult zebrafish. J Comp Neurol 520:933-951.
883 Kyritsis N, Kizil C, Zocher S, Kroehne V, Kaslin J, Freudenreich D, Iltzsche A,
884 Brand M (2012) Acute inflammation initiates the regenerative response
885 in the adult zebrafish brain. Science 338:1353-1356.
886 Lam CS, Korzh V, Strahle U (2005) Zebrafish embryos are susceptible to the
887 dopaminergic neurotoxin MPTP. Eur J Neurosci 21:1758-1762.
888 Lambert AM, Bonkowsky JL, Masino MA (2012) The conserved dopaminergic
889 diencephalospinal tract mediates vertebrate locomotor development in
890 zebrafish larvae. J Neurosci 32:13488-13500.
891 Matsui H, Sugie A (2017) An optimized method for counting dopaminergic
892 neurons in zebrafish. PLoS One 12:e0184363.
893 McLean DL, Fetcho JR (2004a) Relationship of tyrosine hydroxylase and
894 serotonin immunoreactivity to sensorimotor circuitry in larval zebrafish.
895 J Comp Neurol 480:57-71.
896 McLean DL, Fetcho JR (2004b) Ontogeny and innervation patterns of
897 dopaminergic, noradrenergic, and serotonergic neurons in larval
898 zebrafish. J Comp Neurol 480:38-56.
899 McPherson AD, Barrios JP, Luks-Morgan SJ, Manfredi JP, Bonkowsky JL,
900 Douglass AD, Dorsky RI (2016) Motor Behavior Mediated by

Continuously Generated Dopaminergic Neurons in the Zebrafish Hypothalamus Recovers after Cell Ablation. Curr Biol 26:263-269.

Novak M, Vetvicka V (2008) Beta-glucans, history, and the present: immunomodulatory aspects and mechanisms of action. J Immunotoxicol 5:47-57.

Ohnmacht J, Yang Y, Maurer GW, Barreiro-Iglesias A, Tsarouchas TM, Wehner D, Sieger D, Becker CG, Becker T (2016) Spinal motor neurons are regenerated after mechanical lesion and genetic ablation in larval zebrafish. Development 143:1464-1474.

Pappas SS, Tiernan CT, Behrouz B, Jordan CL, Breedlove SM, Goudreau JL, Lookingland KJ (2010) Neonatal androgen-dependent sex differences in lumbar spinal cord dopamine concentrations and the number of A11 diencephalospinal dopamine neurons. J Comp Neurol 518:2423-2436.

Parish CL, Beljajeva A, Arenas E, Simon A (2007) Midbrain dopaminergic neurogenesis and behavioural recovery in a salamander lesion-induced regeneration model. Development 134:2881-2887.

Peron S, Berninger B (2015) Reawakening the sleeping beauty in the adult brain: neurogenesis from parenchymal glia. Curr Opin Genet Dev 34:46-53.

Ramachandran R, Reifler A, Parent JM, Goldman D (2010) Conditional gene expression and lineage tracing of tuba1a expressing cells during zebrafish development and retina regeneration. J Comp Neurol 518:4196-4212.

924 Reimer MM, Sorensen I, Kuscha V, Frank RE, Liu C, Becker CG, Becker T
925 (2008) Motor neuron regeneration in adult zebrafish. J Neurosci
926 28:8510-8516.
927 Reimer MM, Norris A, Ohnmacht J, Patani R, Zhong Z, Dias TB, Kuscha V,
928 Scott AL, Chen YC, Rozov S, Frazer SL, Wyatt C, Higashijima S,
929 Patton EE, Panula P, Chandran S, Becker T, Becker CG (2013)
930 Dopamine from the Brain Promotes Spinal Motor Neuron Generation
931 during Development and Adult Regeneration. Dev Cell 25:478-491.
932 Ronchetti S, Migliorati G, Bruscoli S, Riccardi C (2018) Defining the role of
933 glucocorticoids in inflammation. Clinical science (London, England :
934 1979) 132:1529-1543.
935 Sallinen V, Torkko V, Sundvik M, Reenila I, Khrustalyov D, Kaslin J, Panula P
936 (2009) MPTP and MPP+ target specific aminergic cell populations in
937 larval zebrafish. J Neurochem 108:719-731.
938 Scerbina T, Chatterjee D, Gerlai R (2012) Dopamine receptor antagonism
939 disrupts social preference in zebrafish: a strain comparison study.
940 Amino Acids 43:2059-2072.
941 Skaggs K, Goldman D, Parent JM (2014) Excitotoxic brain injury in adult
942 zebrafish stimulates neurogenesis and long-distance neuronal
943 integration. Glia 62:2061-2079.
944 Stewart A, Gaikwad S, Kyzar E, Green J, Roth A, Kalueff AV (2012) Modeling
945 anxiety using adult zebrafish: a conceptual review. Neuropharmacology
946 62:135-143.
947 Tay TL, Ronneberger O, Ryu S, Nitschke R, Driever W (2011)
948 Comprehensive catecholaminergic projectome analysis reveals single-

949 neuron integration of zebrafish ascending and descending
950 dopaminergic systems. Nat Commun 2:171.
951 Than-Trong E, Ortica-Gatti S, Mella S, Nepal C, Alunni A, Bally-Cuif L (2018)
952 Neural stem cell quiescence and stemness are molecularly distinct
953 outputs of the Notch3 signalling cascade in the vertebrate adult brain.
954 Development 145.
955 Thirumalai V, Cline HT (2008) Endogenous dopamine suppresses initiation of
956 swimming in pre-feeding zebrafish larvae. J Neurophysiol.
957 Tieu K (2011) A guide to neurotoxic animal models of Parkinson's disease.
958 Cold Spring Harbor perspectives in medicine 1:a009316.
959 Tran S, Nowicki M, Muraleetharan A, Chatterjee D, Gerlai R (2016)
960 Neurochemical factors underlying individual differences in locomotor
961 activity and anxiety-like behavioral responses in zebrafish. Prog
962 Neuropsychopharmacol Biol Psychiatry 65:25-33.
963 Vijayanathan Y, Lim FT, Lim SM, Long CM, Tan MP, Majeed ABA,
964 Ramasamy K (2017) 6-OHDA-Lesioned Adult Zebrafish as a Useful
965 Parkinson's Disease Model for Dopaminergic Neuroregeneration.
966 Neurotoxicity research 32:496-508.
967 Wang Y, Li S, Liu W, Wang F, Hu LF, Zhong ZM, Wang H, Liu CF (2016)
968 Vesicular monoamine transporter 2 (Vmat2) knockdown elicits anxiety-
969 like behavior in zebrafish. Biochem Biophys Res Commun 470:792-
970 797.
971 Westerfield M (2000) The zebrafish book: a guide for the laboratory use of
972 zebrafish (*Danio rerio*), 4th Edition. Eugene: University of Oregon
973 Press.

974 Wyatt C, Ebert A, Reimer MM, Rasband K, Hardy M, Chien CB, Becker T,
975 Becker CG (2010) Analysis of the astray/robo2 zebrafish mutant
976 reveals that degenerating tracts do not provide strong guidance cues
977 for regenerating optic axons. J Neurosci 30:13838-13849.
978 Xi Y, Yu M, Godoy R, Hatch G, Poitras L, Ekker M (2011) Transgenic
979 zebrafish expressing green fluorescent protein in dopaminergic
980 neurons of the ventral diencephalon. Dev Dyn 240:2539-2547.
981

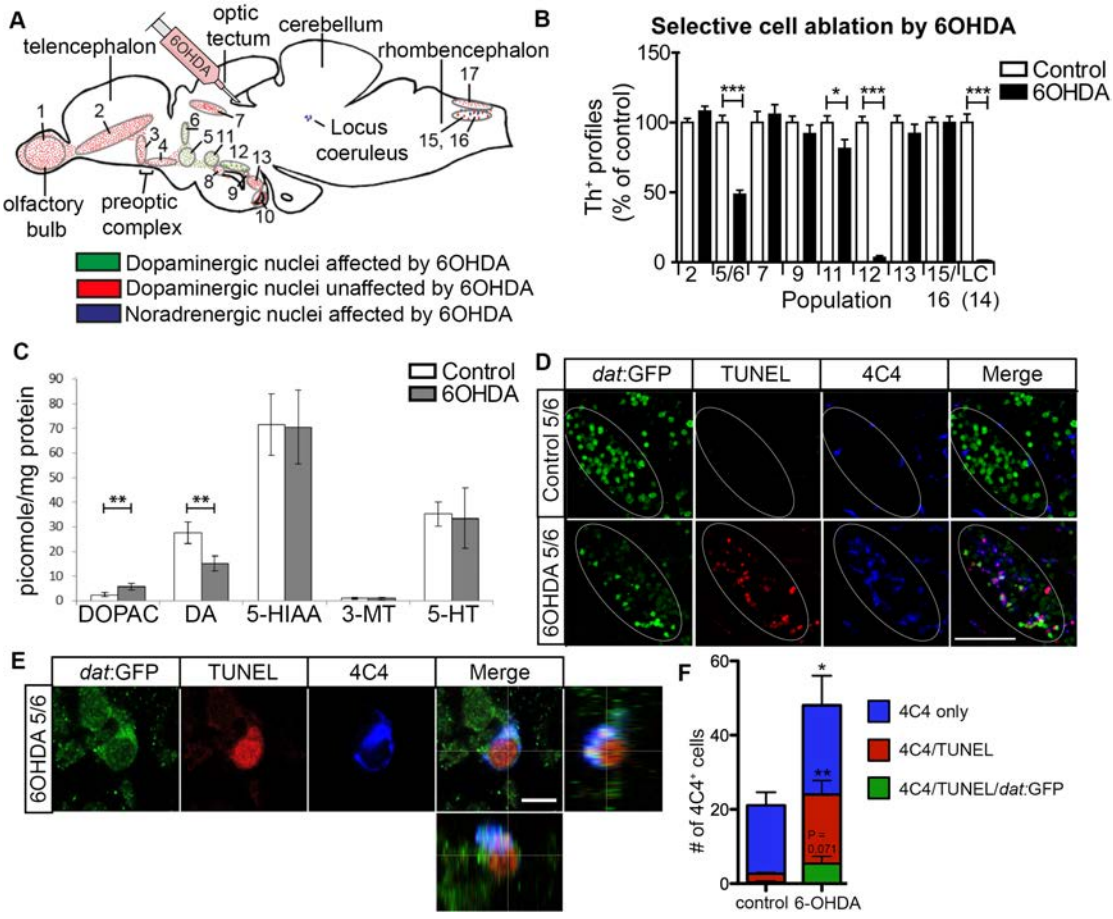

Fig. 1 Specific populations of Th$^+$ neurons are ablated by 6OHDA. **A:** A schematic sagittal section of the adult brain is shown with the 6OHDA resistant dopaminergic cell populations (red) and the vulnerable dopaminergic (green) and noradrenergic populations (purple) in relation to the injection site in the third ventricle indicated. **B:** Quantification of cell loss after toxin injection at 2 dpi is shown. **C:** Injection of the toxin decreases levels of dopamine (DA), increases levels of the metabolite DOPAC, but leaves serotonin (5-HT) and metabolites (5-HIAA, 3-MT) unaffected, as shown by HPLC. **D:** Sagittal sections of population 5/6 are shown in a *dat*:GFP transgenic fish. This shows elevated TUNEL and microglia labelling in population 5/6 after ablation. Note

995 that areas of elevated TUNEL and microglial labelling follow the outlines of the
996 *dat*:GFP+ cell population (ellipse) in the 6OHDA treated animals, but not
997 controls, indicating localised labelling. **E:** A high magnification is shown of a
998 $TUNEL^+$/*dat*:GFP^+ dopaminergic neuron that is engulfed by a $4C4^+$ microglial
999 process (lateral and orthogonal views). **F:** Quantification of microglial cells
1000 inside the 5/6 population (one 50 µm section through 5/6 population from
1001 three animals each) is shown, with subgroups as indicated. Student's T-test
1002 (with Welch's correction for heteroscedastic data) and Mann Whitney-U tests
1003 were used for pairwise comparisons in B, C, F (*$p < 0.05$; ** $p < 0.01$; *** $p <$
1004 0.001). Bar in D = 50 µm, in E = 5 µm.
1005

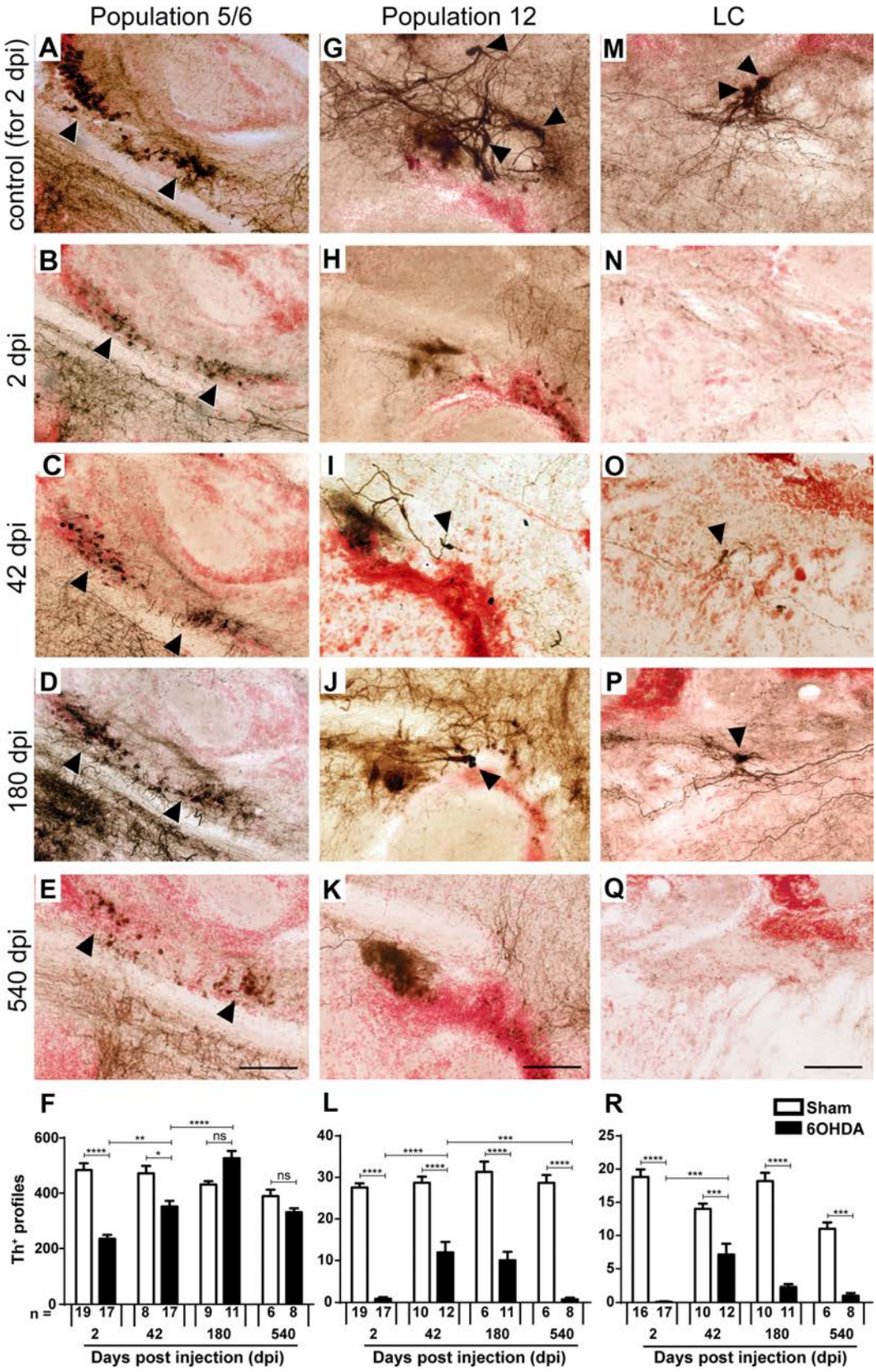

Fig. 2 Replacement of Th$^+$ neurons differs between brain nuclei. Sagittal brain sections are shown; dorsal is up, rostral is left. Some Th$^+$ cell bodies are

indicated by arrowheads. The most representative images are shown, but quantifications are from 1 to 3 tissue sections (50 µm thickness), depending on the extend of the populations. **A-F:** In population 5/6 the number of Th^+ cells is reduced after toxin-induced ablation and back to levels seen in controls without ablation by 180 dpi. **G-L:** In population 12, a partial and transient recovery in the number of Th^+ cells was observed at 42 dpi. **M-R:** In the LC there was also a partial and transient recovery of Th^+ cell number. Note that example photomicrographs of controls are only shown for 2 dpi for clarity reasons, but all statistics were done with age-matched controls. Two-way ANOVA ($p < 0.0001$) with Bonferroni post-hoc test (*$p < 0.05$, **$p < 0.01$, ***$p < 0.001$, ****$p < 0.0001$) for F, L, and R. Bars = 50 µm.

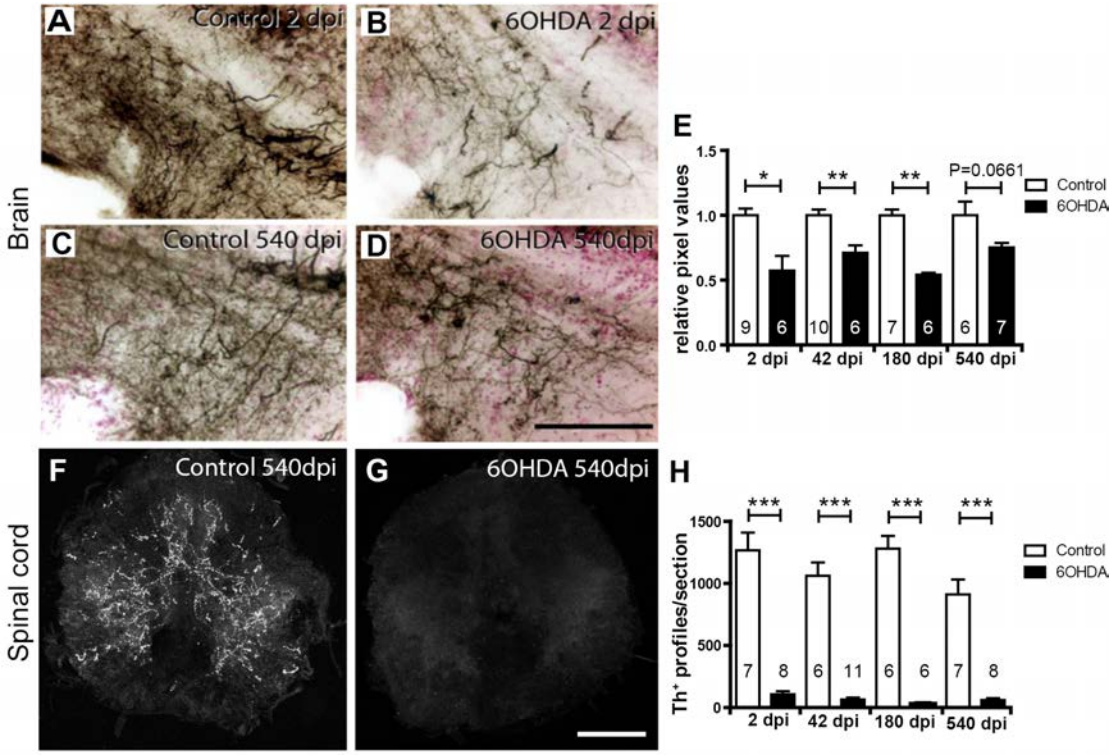

Fig. 3 Th$^+$ axons are inefficiently regenerated. **A-D:** Immunohistochemical detection of Th$^+$ axons (black on red counterstain) in sagittal sections through a terminal field of TH$^+$ axons ventral to population 5/6 is shown. Compared to controls (A), density of these axons is reduced at 2 dpi (B), and is more similar to age-matched controls (C) at 540 dpi (D). **E:** Semi-quantitative assessment of labelling intensity in the area depicted in A-E indicates significant loss of innervation at all time points except the latest, 540 dpi. **F,G:** Spinal cross sections are shown. Compared to age-matched controls (F), immunofluorescence for Th is very low at 540 dpi (G). **H:** Quantification of spinal Th$^+$ axons indicates a lack of regeneration of the spinal projection. Student's T-tests (with Welch's correction for heteroscedastic data) or Mann-Whitney U tests were used for pairwise comparisons as appropriate (*$p < 0.05$; ** $p < 0.01$; *** $p < 0.001$). Bar in D = 100 µm for A-D; bar in G = 100 µm for F,G.

1037

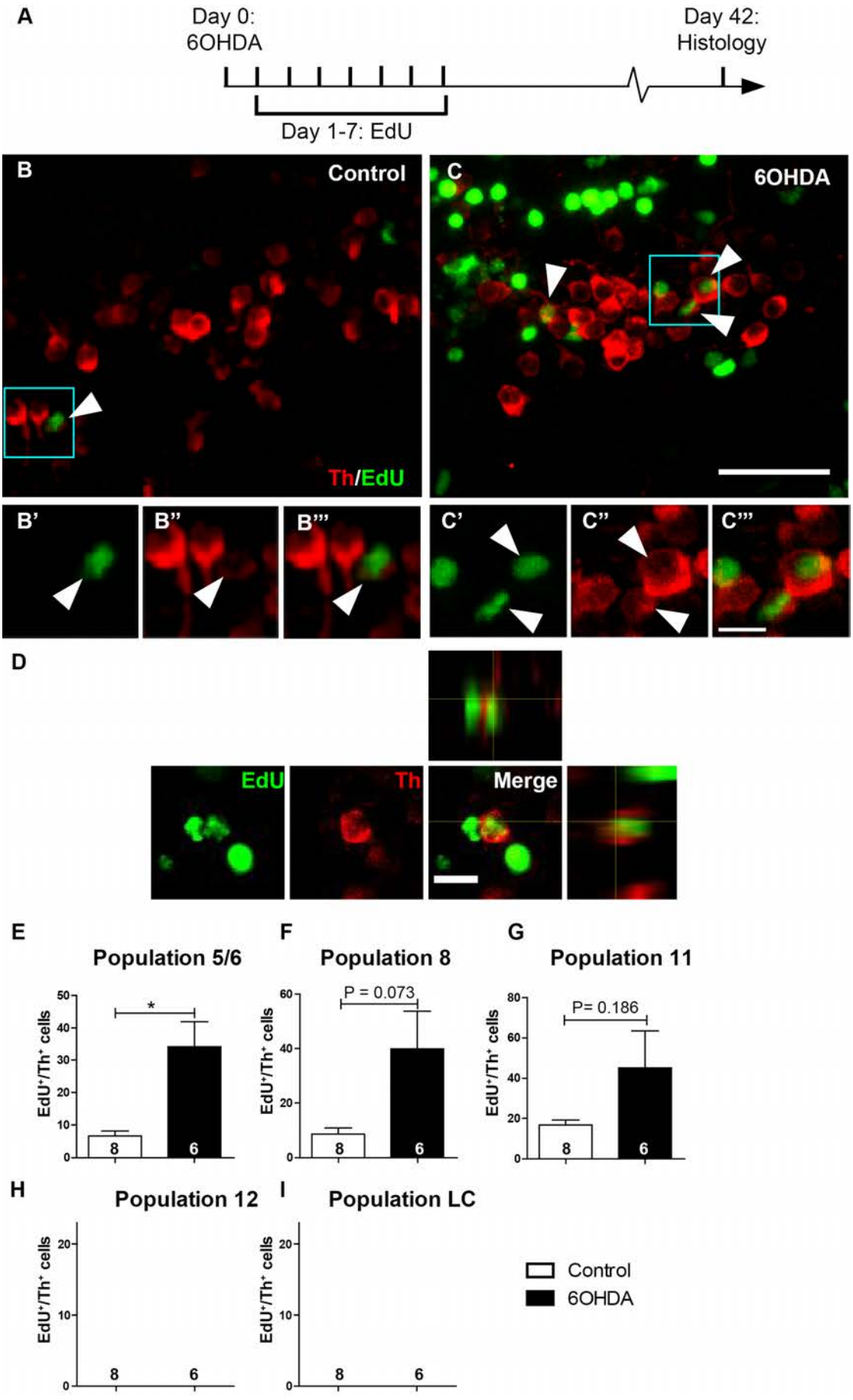
A
Day 0:
6OHDA
Day 42:
Histology
Day 1-7: EdU
B
Control
Th/EdU
C
6OHDA
B'
B''
B'''
C'
C''
C'''
D
EdU
Th
Merge
E
Population 5/6
EdU+/Th+ cells
*
8
6
F
Population 8
P = 0.073
G
Population 11
P= 0.186
H
Population 12
I
Population LC
Control
6OHDA

1038

Fig. 4 Generation of new Th^+ cells is enhanced by prior ablation only in dopaminergic populations showing constitutive neurogenesis. **A:** The experimental timeline is given. **B,C:** In sagittal sections of population 5/6 (rostral left; dorsal up), EdU and Th double-labelled cells can be detected. Boxed areas are shown in higher magnifications in B'-C''', indicating cells with an EdU labelled nucleus, which is surrounded by a Th^+ cytoplasm (arrowheads). **D:** A high magnification and orthogonal views of an EdU^+/Th^+ cell after 6OHDA treatment is shown. **E-I:** Quantifications indicate the presence of newly generated Th^+ cells in specific dopaminergic brain nuclei (E-G). After 6OHDA treatment, a statistically significant increase in the number of these cells was observed for population 5/6. Note that population 12 and LC showed no constitutive or ablation-induced EdU labelled Th^+ cells (H, I). (Student's T-tests with Welch's correction, *$p < 0.05$,). Bar in C = 20 µm for A,B; bar in C''' = 5 µm for B'- C''', bar in D = 10µm.

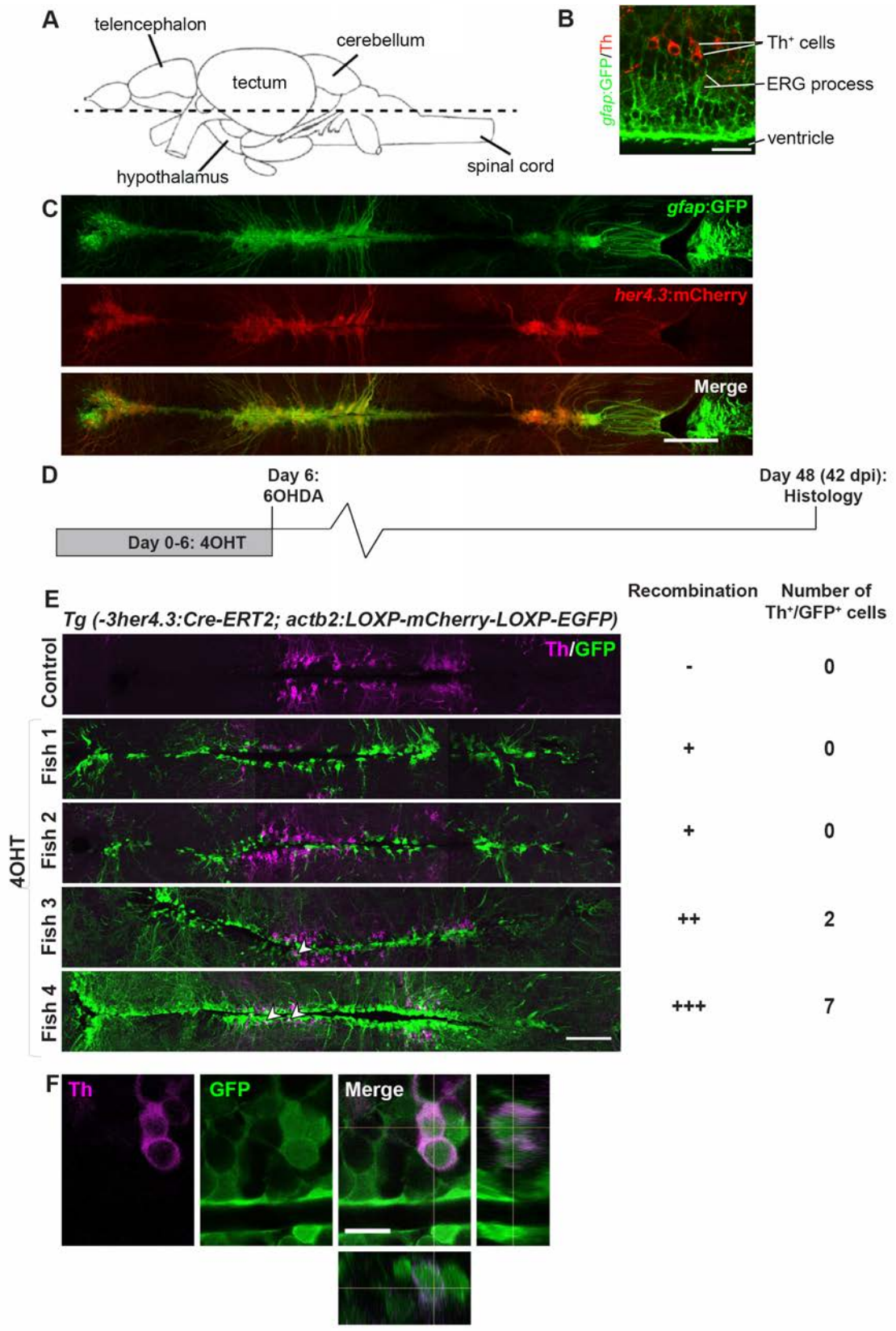
A
telencephalon
cerebellum
tectum
hypothalamus
spinal cord
B
gfap:GFP/Th
Th+ cells
ERG process
ventricle
C
gfap:GFP
her4.3:mCherry
Merge
D
Day 6:
6OHDA
Day 48 (42 dpi):
Histology
Day 0-6: 4OHT
E
Tg (-3her4.3:Cre-ERT2; actb2:LOXP-mCherry-LOXP-EGFP)
Recombination
Number of Th+/GFP+ cells
4OHT
Control
Th/GFP
-
0
Fish 1
+
0
Fish 2
+
0
Fish 3
++
2
Fish 4
+++
7
F
Th
GFP
Merge

1055

1056

1057 Fig. 5 Genetic lineage tracing identifies ERGs as source for new Th$^+$ cells. **A:**
1058 The horizontal section level of all photomicrographs is indicated (rostral is
1059 left). **B:** Th$^+$ cells are in close vicinity to *gfap*:GFP$^+$ processes near the brain
1060 ventricle. **C:** *her4.3*:mCherry$^+$ cells largely overlap with *gfap*:GFP labelling in
1061 double-transgenic animals. **D,E:** Pulse-chase lineage tracing driven by *her4.3*
1062 indicates variable recombination and labelling of mainly ERGs and some Th$^+$
1063 neurons. **F:** High magnification and orthogonal views indicate Th$^+$/GFP$^+$ cells.
1064 Scale bars: in B = 25 µm, C and E = 100 µm; in F = 10 µm.
1065

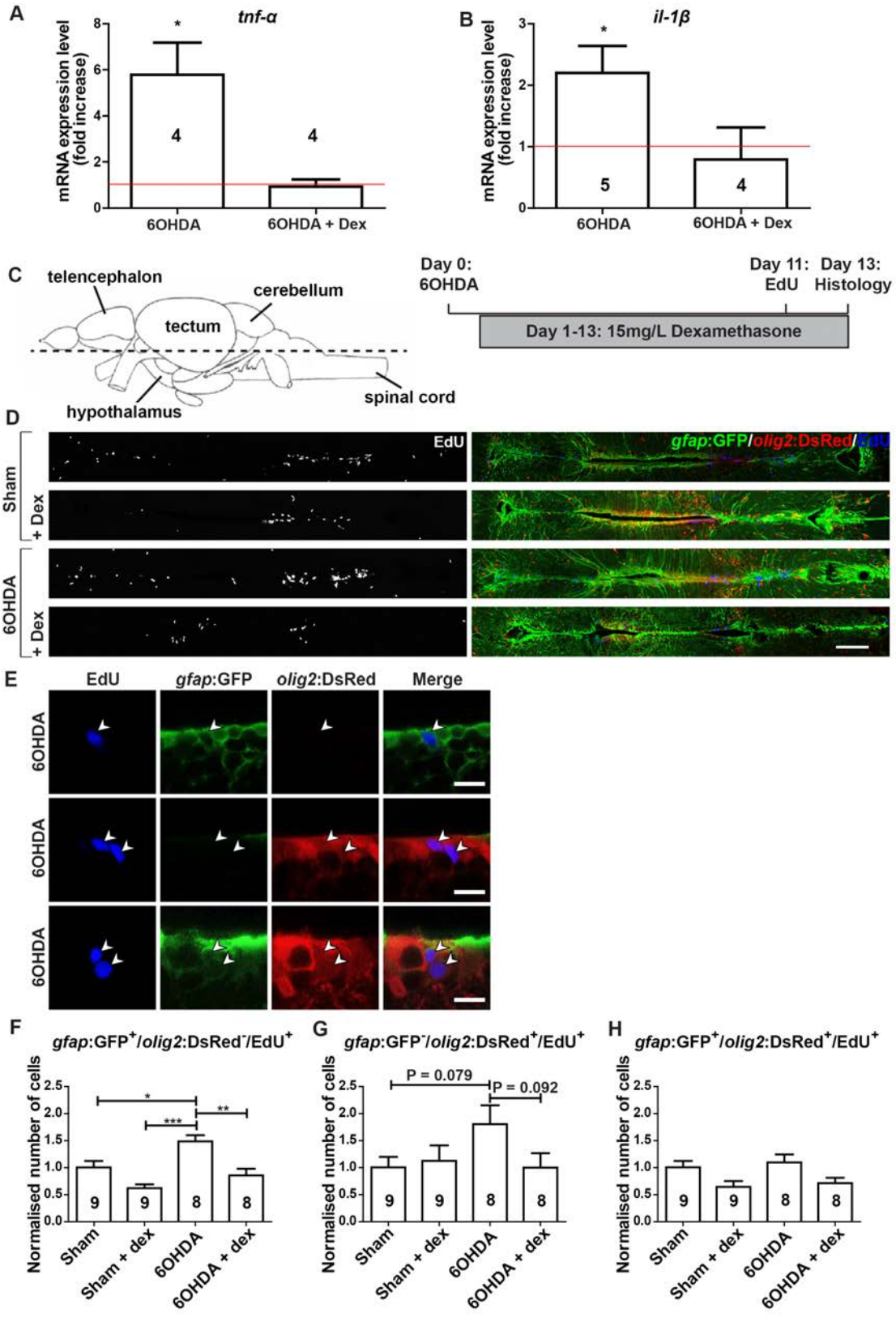

Fig. 6 6OHDA injection increases ERG proliferation, which is abolished by dexamethasone treatment. **A,B:** Levels of *il-1β* (A) and *tnf*-α (B) are increased

by 6OHDA treatment at 3 dpi, but not in the presence of dexamethasone, as shown by qRT-PCR. Each condition is normalised to sham-injected fish (shown by the red line; one-tailed one-sample t-tests, *p < 0.05). **C:** The section level of photomicrographs (left) and experimental timeline (right) are given for D-H. **D:** Overviews of the quantification areas are given. **E:** Higher magnifications of ventricular cells are given. EdU labels ERGs that are only *gfap*:GFP$^+$ (top row), only *olig2*:DsRed$^+$ (middle row) or *gfap*:GFP$^+$/*olig2*:DsRed$^+$ (bottom row) are indicated by arrowheads. **F-H:** The proliferation rate in only *gfap*:GFP$^+$ ERGs is increased by 6OHDA injection and brought back to control levels by dexamethasone treatment (F). A similar non-significant trend is observed for only *olig2*:GFP$^+$ ERGs (G), but not for double-labelled ERGs (H). To facilitate comparisons between the different populations of ERGs, changes induced by the treatments are normalized to the sham-injected group for each population. For F-H: One-way ANOVA with Bonferroni post-hoc test, *p < 0.05, **p < 0.01, ***p<0.001. Scale bars in D = 100 µm; in E = 10 µm.

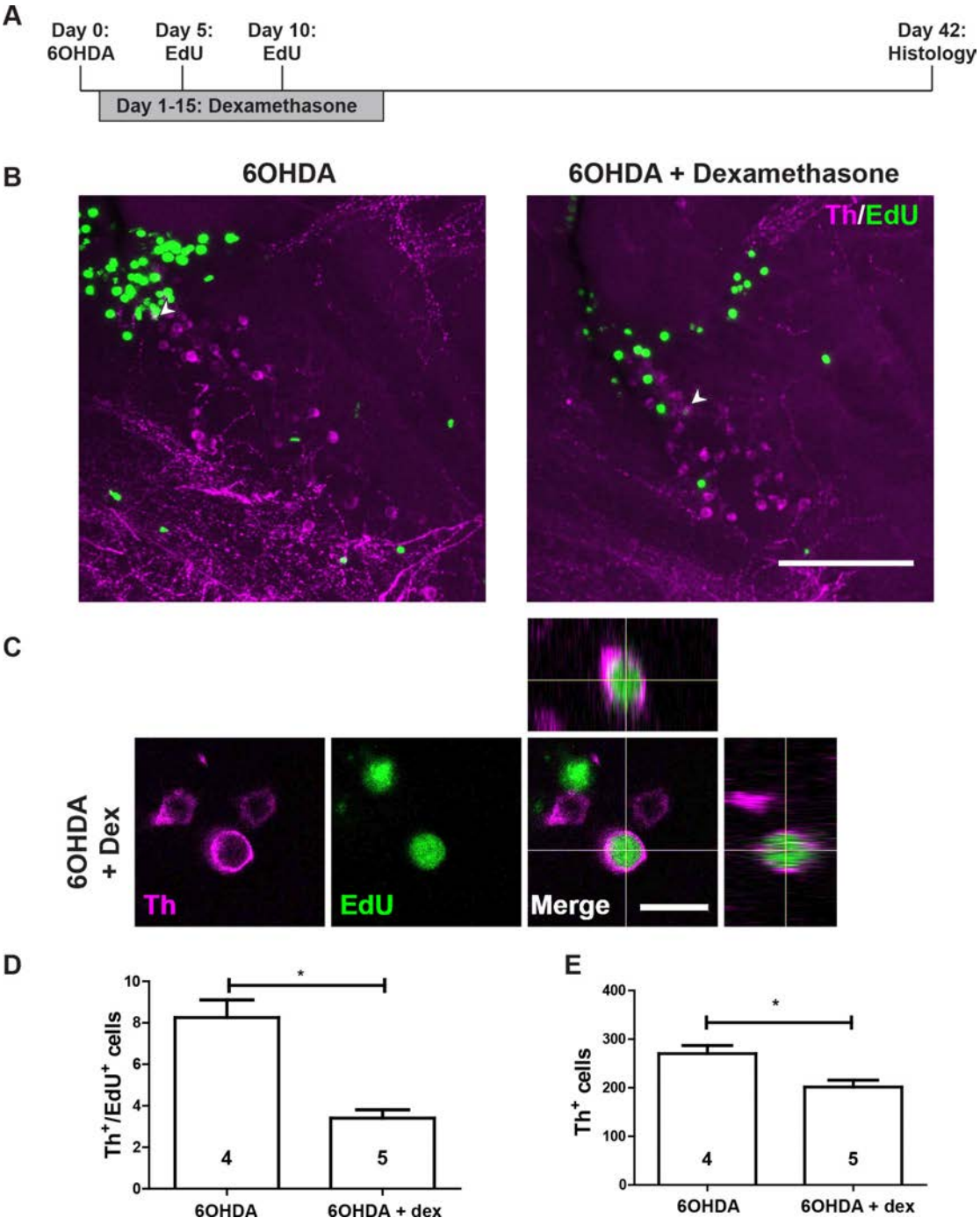

Fig. 7 Dexamethasone inhibits regeneration of Th^+ neurons in the 5/6 population. **A:** The experimental timeline is given. **B:** In sagittal sections of population 5/6, EdU^+/Th^+ neurons are present (arrowheads) after 6OHDA

injection, with (left) or without addition of dexamethasone (right). **C:** High magnification and orthogonal views of an EdU^+/Th^+ neuron are shown. **D,E:** The number of EdU^+/Th^+ (D; Mann Whitney-U test, *$p < 0.05$) and the overall number of Th^+ neurons (E; Student's t test, *$p < 0.05$) are reduced by treating 6OHDA-injected animals with dexamethasone. Scale bar in B = 100 µm; in C = 10 µm.

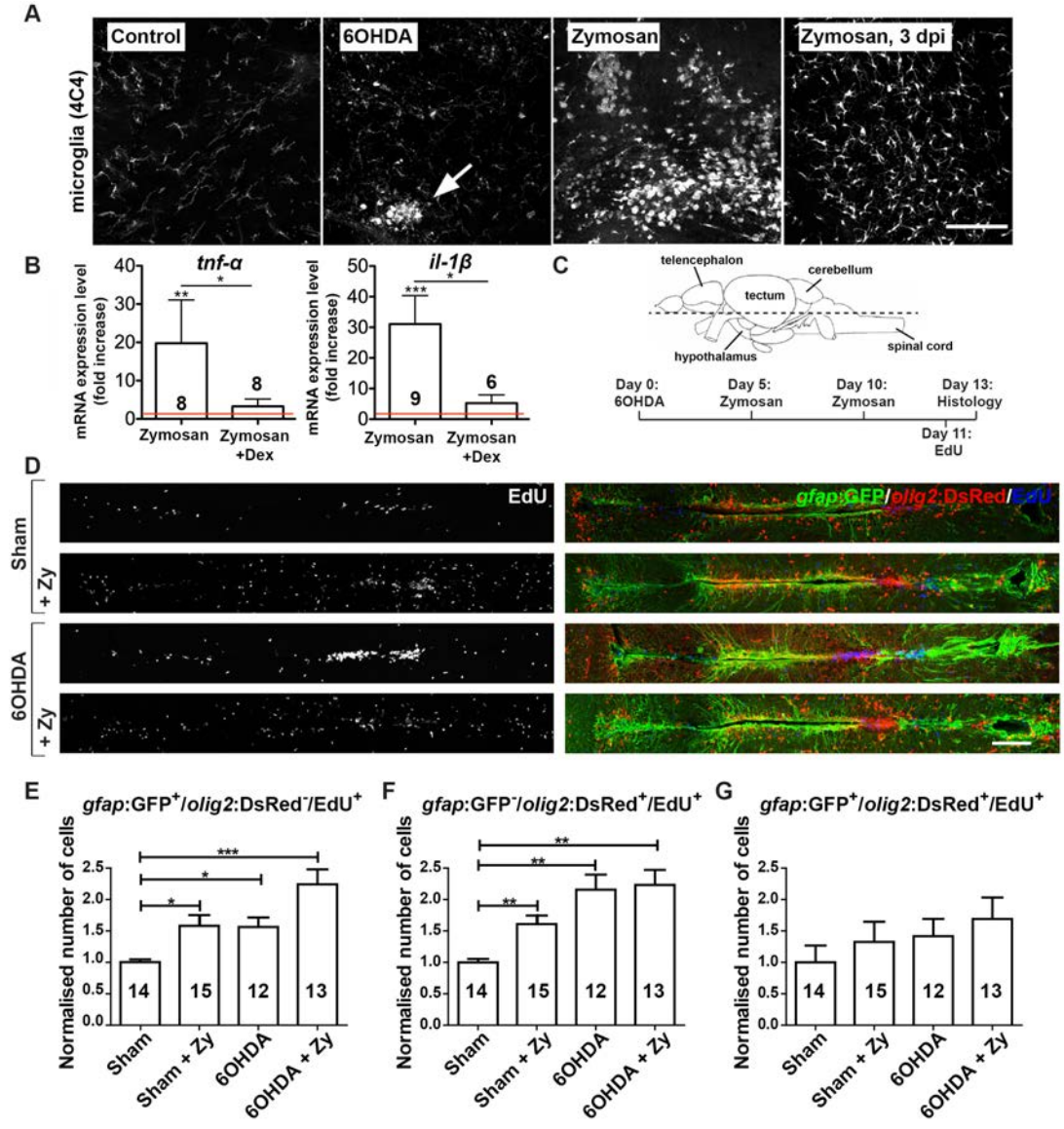

Fig. 8 OHDA and Zymosan injections both increase ERG proliferation. **A:** In sagittal sections of population 5/6 restricted microglia activation at 24 hours after 6OHDA injection (arrow) compared to sham-injected control animals is observed. Zymosan injection leads to much stronger, non-localised microglia response that lasts for at least three days. **B:** Zymosan injection massively increases mRNA levels for *il-1β* and *tnf*-α compared to vehicle-injected controls at 12 hpi. This is inhibited by co-application of dexamethasone (one-

1113 way ANOVA with Dunn's multiple comparisons; *P = 0.035 (for *tnf*-α); *P =
1114 0.0447 (for *il-1β*); **P = 0.0019; ***P = 0.0004) **C:** The horizontal plane of
1115 sectioning (rostral is left for all panels in D) and the experimental timeline for
1116 D-G is shown. **D-G:** 6OHDA injections and Zymosan injections, alone or in
1117 combination, increase proliferation of ERGs (D). This is true for only
1118 *gfap*:GFP^{+} (E) and only *olig2*:DsRed^{+} (F), but not double-labelled ERGs (G).
1119 To facilitate comparisons between the different populations of ERGs, changes
1120 induced by the treatments are normalized to the sham-injected group for each
1121 population. One-way ANOVA with Welch's correction and Games-Howell
1122 post-hoc test for E, F (*$p < 0.05$, **$p < 0.01$, ***$p < 0.001$), one-way ANOVA
1123 for G ($p > 0.05$). Scale bar in A = 100 μm; in D = 100 μm.
1124

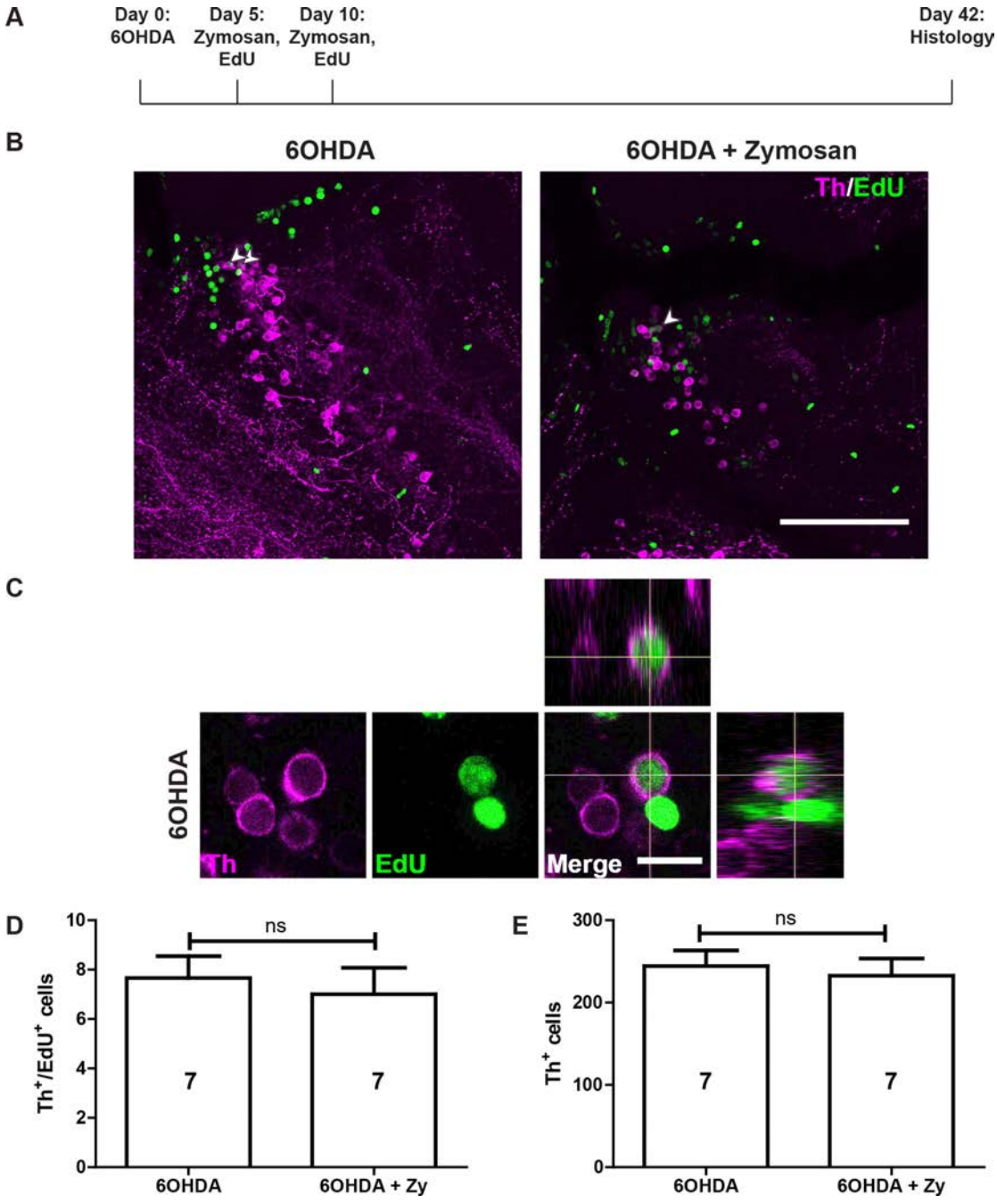

Fig. 9 Zymosan treatment does not augment Th^+ neuron replacement in population 5/6. **A:** The experimental timeline is indicated. **B:** In sagittal sections of population 5/6, Th^+/EdU^+ neurons can be observed (arrowheads) after 6OHDA injection with (right panel) or without addition of Zymosan (left). **C:** High magnification and orthogonal views of an EdU^+/Th^+ neuron are shown. **D,E:** The number of Th^+/EdU^+ (D) and the overall number of Th^+

neurons (E) are not increased by treating 6OHDA-injected animals with Zymosan (Student's T-tests, $p > 0.05$). Scale bar in B = 100 μm; in C = 10 μm.

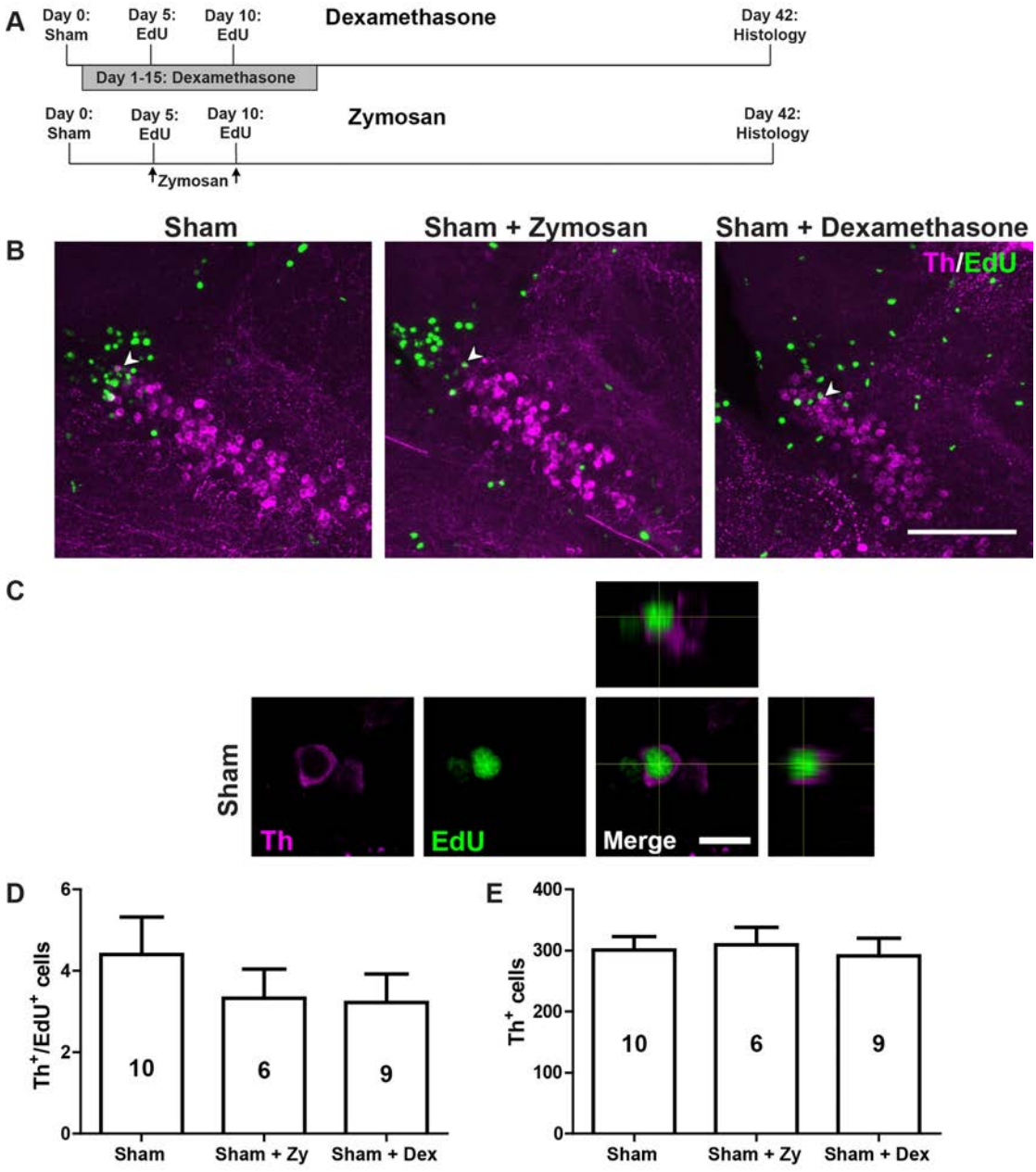

Fig. 10 Immune system manipulations in animals without ablation do not influence addition of new Th^+ cells. **A:** Timelines of experiments with either Zymosan or dexamethasone treatment. **B:** In sagittal sections of population 5/6, Th^+/EdU^+ neurons (arrowheads) can be observed in all experimental conditions. **C:** A high magnification and orthogonal views of a double-labelled neuron in a sham-injected animal are shown. **D,E:** In animals without TH^+ cell ablation, no changes are observed in the number of newly generated Th^+

neurons and the overall number of Th neurons after dexamethasone or Zymosan treatment (One-way ANOVA with Bonferroni post-hoc test used in D and E, $p > 0.05$). Scale bar in B = 100 μm; in C = 10 μm.

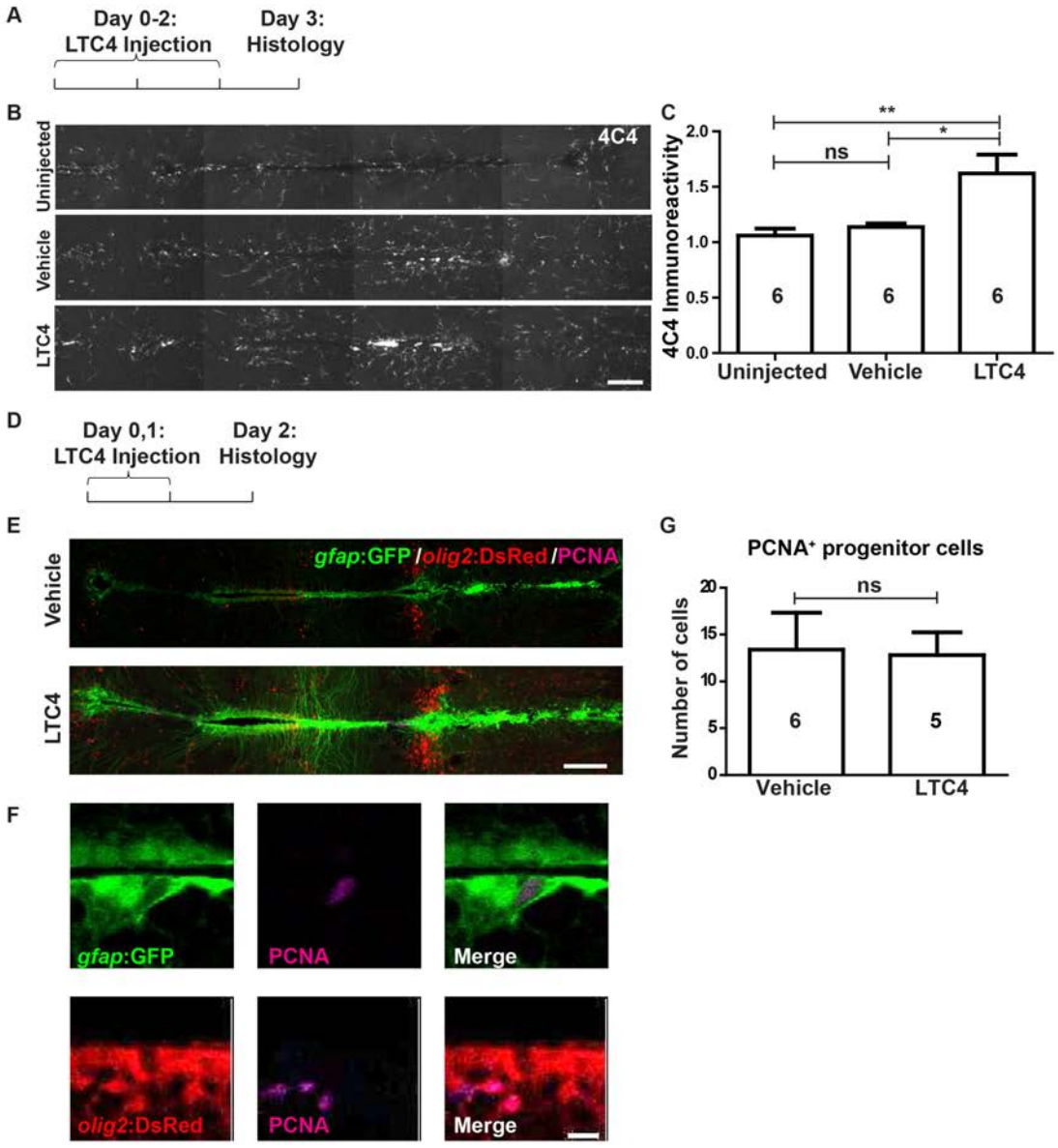

1150

1151 Fig. 11 LTC4 moderately activates microglia but does not increase

1152 proliferation of ERGs. Horizontal sections are shown, rostral is left. **A-C:**

1153 LTC4, but not vehicle injection leads to an increase in microglia labelling in

the brain **D-G:** PCNA labelling in *gfap*:GFP$^+$ and/or *olig2*:DsRed$^+$ ERGs is not increased by LTC4 treatment (One-way ANOVA with Bonferroni post-hoc test used in C, Mann Whitney-U test used in G, *$p < 0.05$). Scale bars = 100 μm in B and E, 10 μm in F.

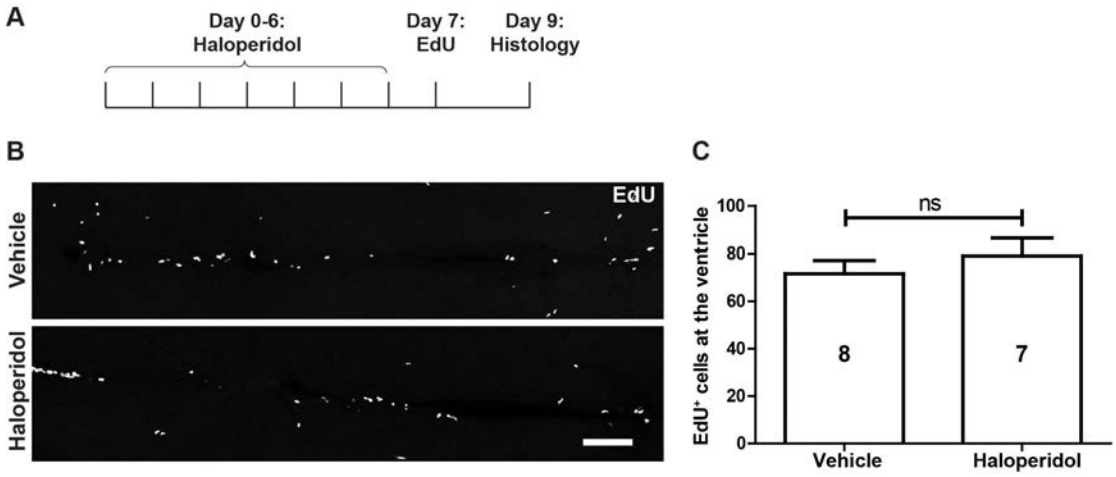

Fig. 12 Inhibition of dopamine signalling does not affect ERG proliferation. **A:** The experimental timeline for B,C is shown. **B,C:** Horizontal sections (B) and quantification (C) show no effect of Haloperidol on proliferation in the ERG layer. (Student's t-test, $p > 0.05$). Scale bar in B = 100 µm.

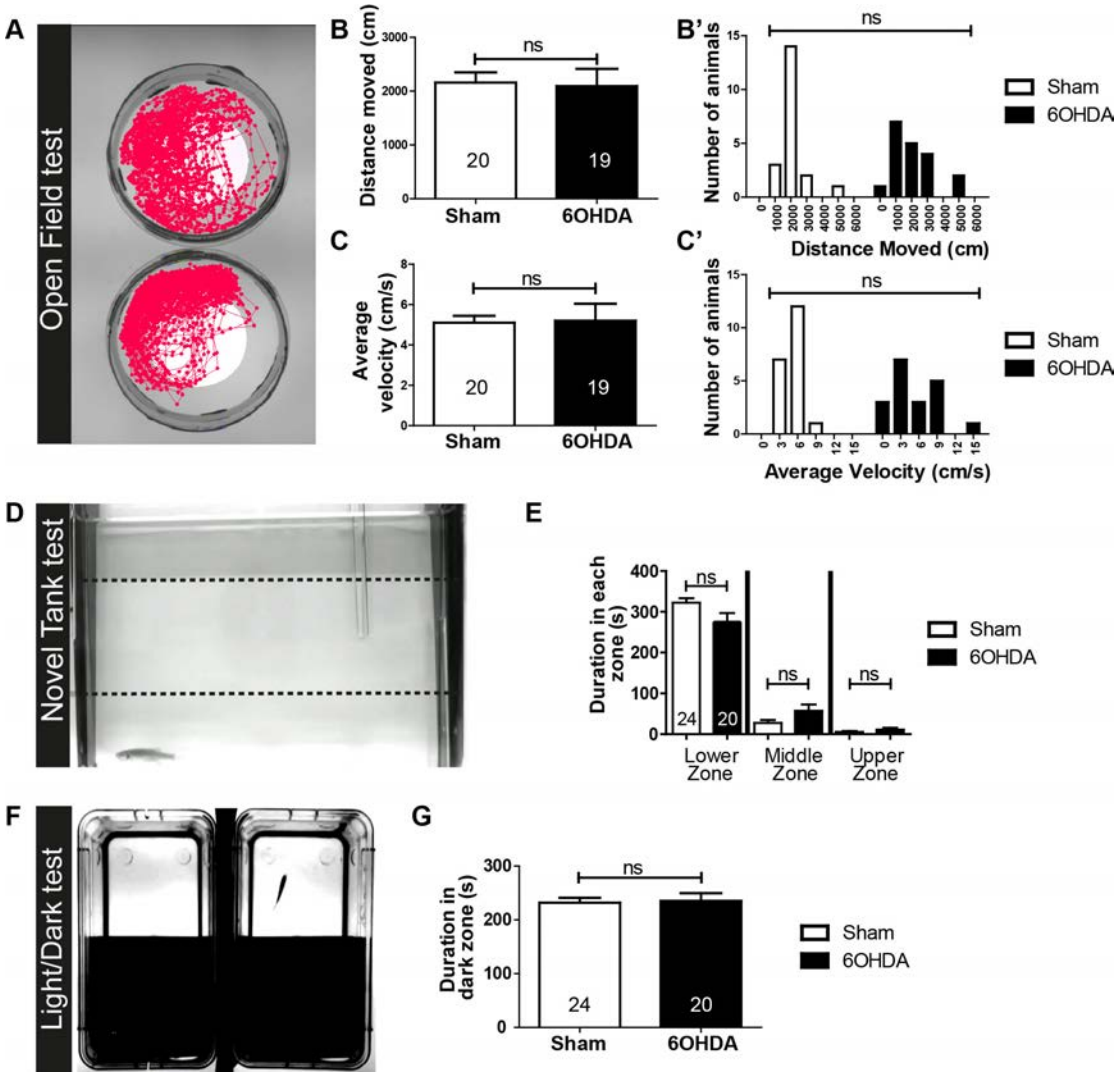

Fig. 13: Basic swimming parameters and anxiety-like behaviours are unaltered by 6OHDA treatment. **A-C:** Typical swim tracks are shown (A). Quantifications of averages (B,C) and frequency distributions (B',C') of distance swum (B) and average velocity (C) show no differences between control and treated fish (Student's T-test, $p > 0.05$ for B and C; Kolmogorov-Smirnov Test, $p > 0.05$ for B' and C'). **D,E:** A side view of a fish preferring the lower third of a novel tank is shown (D). Quantifications of time spent in the

different depth of the tank (E) show the same preference for the lowest compartment in control and 6OHDA-treated fish (Mann-Whitney U-tests, $p > 0.05$). **F,G:** The setup for the light/dark preference test is shown from above (F). Quantifications (G) indicate that control and treated fish do not differ in their preference for the dark compartment in a 300 seconds observation period (Student's T-test, $p > 0.05$).

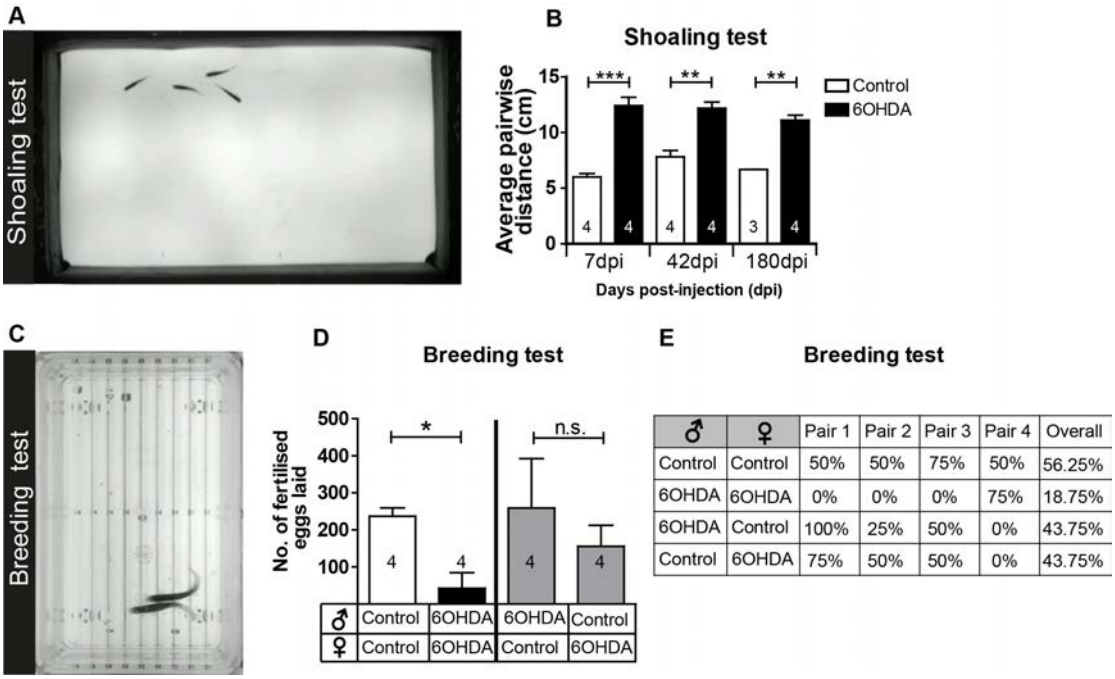

♂	♀	Pair 1	Pair 2	Pair 3	Pair 4	Overall
Control	Control	50%	50%	75%	50%	56.25%
6OHDA	6OHDA	0%	0%	0%	75%	18.75%
6OHDA	Control	100%	25%	50%	0%	43.75%
Control	6OHDA	75%	50%	50%	0%	43.75%

Fig. 14 Injection of 6OHDA permanently impairs shoaling behaviour and decreases mating success. **A,B:** Shoaling behaviour as viewed from above in shallow water is shown in A. The average pairwise distance of fish from each other is significantly increased at all time points tested (Student's T-tests with Welch's correction for heteroscedastic data were used for pairwise comparisons; *p < 0,05, **p < 0.01, ***p < 0.001). N-numbers indicate number of shoals of 4 fish each. **C-E:** Fish showing mating behaviour are shown from above (C). Clutch sizes (D) and mating success rates (E) are strongly reduced when animals are mated after 6OHDA injection. Mating the same females or males with the same control fish showed that mating success does not depend on lack of 6OHDA in either males or females alone. N-numbers indicate different pairs of fish (D; Mann-Whitney U-tests, P < 0.05).

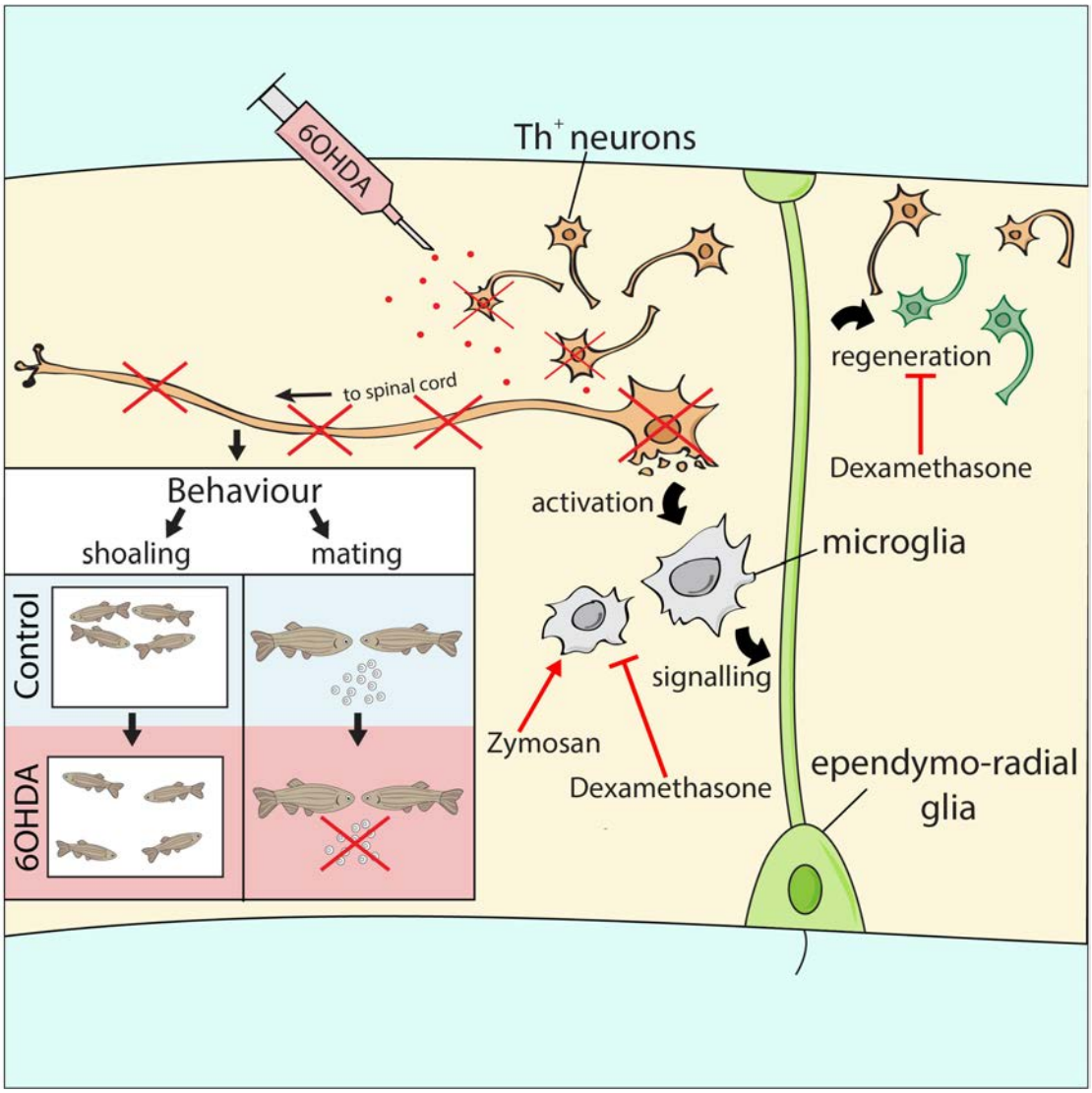

Fig. 15 Schematic overview of results. 6OHDA injection ablates specific Th^+ cell populations, leading to a microglia response, which is necessary for regeneration of new dopaminergic neurons from ERGs. This is blocked by dexamethasone, whereas Zymosan stimulates ERG proliferation, but not addition of Th^+ neurons. Neurons projecting to the spinal cord are not replaced, associated with deficits in shoaling and mating behaviours.